Chapter 2
Microfluidics Overview

Geeta Bhatt, Sanjay Kumar, Poonam Sundriyal, Pulak Bhushan, Aviru Basu, Jitendra Singh, and Shantanu Bhattacharya

1 Introduction

Microelectromechanical systems and micro-fluidics are two fast emerging domains in diagnostics research. The Microsystems technology emerged as a fall out of the microelectronics industry mostly due to the obsoleteness of some of the microelectronic processes owing to integration density issues. The area was first widely explored in the mechanical and physical sensing domains and found wide interests primarily because of low overall size, high yields of production and ability to integrate with a variety of processes. The technology saw a turnaround towards chemical/biochemical sensing starting from the end of 80s as prompted by the fast molecular diagnostic requirements imposed by the gene sequencing industry fuelled by the Human Genome project. Microfluidics is mostly concerned with handling of miniscule samples of fluids of volume 10^{-9}–10^{-18} L which is well suited to the handling of different expensive analytes important for diagnostics

G. Bhatt • S. Kumar • P. Sundriyal • P. Bhushan • J. Singh
Microsystems Fabrication Laboratory, Kanpur, Uttar Pradesh, India

Department of Mechanical Engineering, Indian Institute of Technology, Kanpur, Uttar Pradesh, India

A. Basu
Microsystems Fabrication Laboratory, Kanpur, Uttar Pradesh, India

Design Programme, Indian Institute of Technology, Kanpur, Uttar Pradesh, India

S. Bhattacharya (✉)
Microsystems Fabrication Laboratory, Kanpur, Uttar Pradesh, India

Department of Mechanical Engineering, Indian Institute of Technology, Kanpur, Uttar Pradesh, India

Design Programme, Indian Institute of Technology, Kanpur, Uttar Pradesh, India
e-mail: bhattacs@iitk.ac.in

C.K. Dixit, A. Kaushik (eds.), *Microfluidics for Biologists*,
DOI 10.1007/978-3-319-40036-5_2

work. This technology has very prominent advantage with respect to low overall chip area and high integration density. For handling small volumes of fluid of the range indicated above various micro-channels and micro-confinements are devised using a variety of techniques in which the mixing, reacting, handling and transporting etc. take place. The main motivations of this field are powerful analytical and diagnostic techniques which have been parallel devised by chemists, biochemists and material scientists over the last couple of decades to understand the life processes for sustenance of life itself. These may include modern methods as used in chemical diagnostics like [1]:

1. Micro-analytical methods (Chemical analysis methods for higher sensitivity and higher resolution)
   (a) High-pressure liquid chromatography (HPLC)
   (b) Matrix assisted laser desorption/ionization time of flight methods (MALDI-TOF)
   (c) Capillary electro-osmosis and electrophoresis methods (CE)
2. Sensitive detection of for chemical and biological hazards which may have military connotations (being used as bio-warfare tools)
3. Molecular biology driven methods to recognize basic structures of biological entities deterministically which may include:
   (a) High throughput DNA sequencing
   (b) Causative genomics
   (c) Protein crystallography and folding
   (d) Immunological mechanisms through the study of binding chemistries of various pathogenic and non-pathogenic biological entities so on so forth

The fluid which is analysed in the microfluidics domain can be handled in various ways. Hence depending on this, microfluidics is classified in three different types, continuous flow microfluidics (in which there is continuous flow of fluid through the micro-channels), droplet based microfluidics (in which discrete manipulating volumes are formed in the immiscible phase) and digital microfluidics (in which discrete, independently controlled droplets are manipulated in the open environment i.e., on the substrate) [2]. Depending upon the requirements, various materials like silicon, glass and various elastomers (polydimethysiloxane (PDMS), SU8 (negative photoresist)) are used in microfluidics for making various micro-channels, micro-valves etc. Hence keeping in view the various requirements of the field of microfluidics, a large domain of researchers are involved in the field pertaining to the advanced applications of the field of Microfluidics.

In recent years, microfluidics has been an extensively explored domain owing to its high applicability to develop low-cost diagnostic devices. Clinical diagnostics is one of the promising application areas for deployment of such lab-on-chip systems also better known as point-of-care (POC) systems [3]. Lab-on-chip technology is preferred over conventional laboratory lab oriented techniques due to their faster performance and overall miniaturized size which leads to reduced use of analytes

and thus promotes low cost clinical diagnostics which can be of immense utility in resource poor settings. Various advantages that such devices offer are reduced detection time, increased sensitivity, greater control of molecular interactions, cost efficiency, reduced chemical wastage, lesser human intervention etc. With a purpose of exploring various dimensions of microfluidics in clinical diagnostics, this chapter summarizes various aspects of the field of point of care diagnostic devices including their fabrication technologies like Laser micro-machining, lithography and MRDI process for making micro-channels/micro-valves; micro-fluidic systems and its various fluid handling modules like micro-mixers, micro-pump, micro-valve and micro-cantilevers etc. various applications of micro-fluidics like electrophoresis (gel electrophoresis, capillary electrophoresis and surface electrophoresis), dielectrophoresis, polymerase chain reaction (PCR) and gene delivery and further various sensing and detection techniques like electrochemical sensing, optical sensing, mass based sensing and surface plasmon resonance (SPR) sensing etc.

2 Basic Fabrication Techniques

In this section we would like to discuss the various fabrication techniques that are normally used for micro-fabrication of high aspect ratio micro-channels.

2.1 LASER

The term LASER is an acronym for Light Amplification by Stimulated Emission of Radiation. Laser devices produce intense light beams which are monochromatic, coherent, and highly collimated. The wavelength of laser light is monochromatic and all photons are coherent. Laser beams show very low divergence and can travel over great distances, can be focused to a very small spot with high intensity and find a variety of applications in different fields.

Atoms possess energies only in particular discreet energy levels although when in bulk there may be a bulk behaviour of the orbital energies. The electrons within these atoms are naturally present in their ground state and they go to higher energy levels when excited through light beams of an external source. This process is known as absorption. After a short duration of time is lapsed the electrons returns back to their initial ground states and in the process the atom emits a photon. This process is known as spontaneous emission. In a traditional light source both absorption and emission occur together. If an outside photon having precisely the amount of energy needed for spontaneous emission is struck on the excited atoms, this external photon is increased to two photons one provided by the excited atom. Both released photons have the exact same phase. This process is known as stimulated emission and it is a fundamental process for the operation of a laser

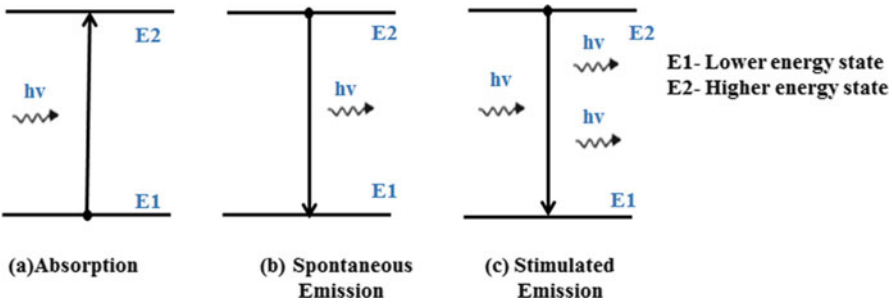

Fig. 2.1 Schematic of Laser process

source (Fig. 2.1). In this process, the key is the photon having exactly the same wavelength as that of the emitted light [4]. Application of laser machining for micro-channel fabrication and mask making is discussed in the following sections.

2.1.1 Application of Laser Machining for micro-channel making

Laser Photo-ablation was first introduced in 1997 by Roberts's group for making polymer microfluidic channels [5]. The integration of laser micro-beams with micro-fluidic devices is beneficial for rapid throughput fabrication strategies particularly for Lab on chip applications to achieve the manipulations of biological entities and biological fluids within micro-fluidic platforms [6, 7]. One specific advantage of pulsed laser micro-beam irradiation is that it does not require any specialized instrumentation except a XYZ stage which would follow commends from a drawing software. This reduces the design complexity and cost of the individual micro-devices tremendously while increasing the speed of their fabrication by several folds. So it is economical to dispose the devices so made after a single use. Secondly, the laser micro-beam can be positioned to any optically accessible location within the micro-device thus provides high flexibility in designs, enables potential parallelization of cellular analysis at multiple device locations etc. [7].

In laser machining processes, a high power laser is used to break the bonds of polymer molecules thereby removing the decomposed polymer parts from the region being ablated by the laser. Excimer laser has been successfully used for making micro-channels with 193 or 248 nm pulses with a pulsing frequency range of 10 to several kilo-hertzs. Micro-channels can be made by a maskless direct laser etching process or through lithographic patterning processes [8]. Laser etching is suitable for machining a wide range of polymeric materials including polymethyl methacrylate (PMMA) [9], polystyrene (PS), polycarbonate (PC), polyethylene terephthalate (PET), polyethylene terephthalate glycol (PETG), polyvinylchloride (PVC) and polyimide [10]. Surface chemistry can be modified due to the formation

of reactive species during the laser ablation process which makes this process very attractive to biological assays.

Laser fabricated channels have high surface roughness than injection molded, imprinted or hot embossed channels although a newly intended hybrid machining strategies particularly on PMMA claims to have an average surface roughness of a few hundred nanometers [11]. Surface roughness depends on the absorption of the lasing frequency of the polymer. For example, PMMA channels made at 248 nm have high roughness and porosity [12]. Parameters to govern quality of the fabricated channels are laser power, scanning speed, polymer absorptivity, laser pulse rate and number of passes made to realize a complete channel.

2.1.2 Application of LASER Machining for Mask Making

Photo-masks are very important for miniaturization of devices. However, due to finite scanning speeds of laser pattern generators this process has an overall low-throughput. MEMS fabrication is typically a multilayer fabrication process when we consider devices and is also highly iterative thus needing multiple changes based on device performance so that the design can achieve finality. Hence precise mask fabrication is a critical step towards the MEMS grade precision and accuracy needs. For making such masks a MEMS laboratory needs a laser pattern generator for easy control on mask- fabrication process [13, 14]. Nonconventional machining has been widely used for micro-machining purposes but their use for mask making is not much explored [15]. Kumar et al. has shown how non-conventional manufacturing processes can be utilized towards the fabrication of small MEMS grade structure [16].

Laser machining is a highly localized and non-contact process to ablate micro-features and structures has three simple steps, viz., (a) interaction between the matter and beam, (b) absorption/heat conduction and an associated temperature rise, and (c) melting and vaporizing of the material. The various advantages as offered by laser micro-machining are the easy and precision control and rapid machining.

Figure 2.2 shows a one-step demagnification and laser ablation technique as applied to mask making as reported by Kumar et al. [16].The aluminium mask which is made with large sized features through electro-discharge machining processes is mounted on the excimer laser system and the shadow the mask is subsequently demagnified on a thin chrome film after proper alignment and focusing. An optimum solution can be extracted from the different machining parameters, including energy, pulse frequency, pulse duration, and pulse numbers, etc., so that edge roughness of fabricated features can be minimized. An energy optimization can also be performed by energy value calculation used for metal film ablation without affecting substrate. The minimum resolvable feature-size using this is roughly 10 μm [16]. The mask-making strategy with a combination of advanced machining technologies, easily available within an advanced machining laboratory, can be very helpful for iterative micro-systems designing.

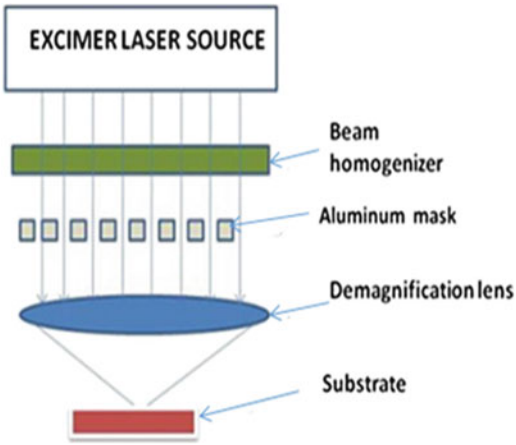

Fig. 2.2 Schematic of the demagnification lens placement after shadow mask [16]

2.2 Photo-Lithography

Photo lithography is a non-contact process which deploys the power of light exposure to print extremely small features (up to sub micron levels) into photo-chemicals and resists. Major steps in optical lithography are pattern transfer, alignment and exposure; which are explained in the forthcoming sections in details.

2.2.1 Pattern Transfer

In lithography processes a pattern is transferred to a photosensitive material by selective exposure to a radiation source (UV source in photolithography, X-Ray source in X-Ray lithography, electron beam in e-beam lithography etc.) (Fig. 2.3). Physical properties of the photosensitive chemical change when it is exposed to such radiation source. The changed properties of the photo-chemical render the exposed regions to be constitutionally different from the unexposed regions and this different created by light is utilized to print features and structures on the surface of the photochemical [17]. The changed properties are different with positive and negative tone photochemicals. In a positive tone resist the exposed regions are debonded and in the negative tone resist these regions are cross-bonded (Fig. 2.4a, b).

If the resist is exposed to a specific wavelength of light the chemical resistance of the resist to developer solution differs. If the resist is placed in a developer solution after selective exposure to a light source, one of the two regions will be etched (exposed or unexposed). If the exposed material is etched away by the developer, the material is positive resist as shown in Fig. 2.4a. If and the unexposed region is etched away, it is considered to be a negative resist as shown in Fig. 2.4b.

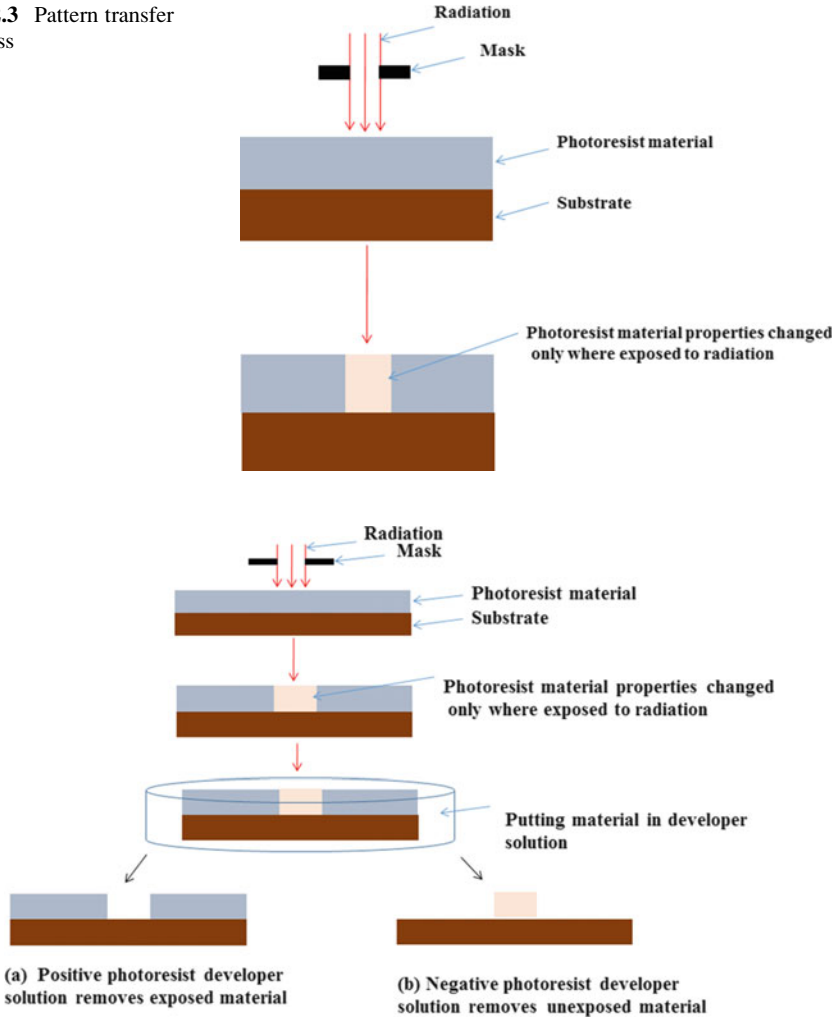

Fig. 2.3 Pattern transfer process

Fig. 2.4 (**a**) Pattern in positive photoresist, (**b**) Pattern in negative photoresist

2.2.2 Alignment

Pattern alignment plays a major role in photo-lithography for making controlled feature sizes and shapes. The pattern transferred to a wafer has a set of alignment marks which have highly precise features. These marks are used as reference for positioning other patterns at different layers with respect to a pattern of one layer each alignment mark should be labelled for easy identification, positioning and time saving [17]. Complex MEMS features are mostly multi-level and use multiple masks for different operations related to micromachining on a single chip platform.

2.2.3 Exposure

The main exposure parameters to achieve accurate pattern transfer from the mask to the photosensitive layer depend on radiation source wavelength and the exposure dose required achieving the desired property change of the photo-resist. Typical sources of UV light are mercury vapour lamps and excimer lasers. A chemical reaction takes place between the light and resist when UV light hits the resist. The mask unprotected areas undergo a chemical reaction [17]. Application of lithography is discussed in the next section.

2.3 Soft Lithography

Soft lithography covers a domain of processes which are based on non-photolithographic techniques principally based on replica moulding and self-assembly processes for micro and nanoscale fabrication. It is a convenient, effective and inexpensive method for making micro and nanostructures. Under the replica moulding process an elastomeric patterned stamp with relief structures on its surface is used to generate patterns with very small features (30–100 μm size) by a casting process using a soft polymeric material called PDMS. Replica Further the patterned polydimethylsiloxane (PDMS) stamps may be used to print molecules on surfaces with great precision and accuracy a process better known as micro-contact printing [18]. In the replica moulding process a silicon master is fabricated with patterned features composed of photoresists which are used for PDMS micro-channel fabrication. Silicon wafers are firstly coated with photoresist and undergo a photolithography step to generate a set of pattern on the surface of the wafer [19, 20].

Replica moulding with PDMS is carried out by pouring PDMS prepolymer (PDMS and curing agent) onto a pretreated (with mold release agent) and patterned Silicon wafer which acts as a mold. To obtain an enclosed micro-fluidic device, the PDMS replica is reversibly or irreversibly sealed to a variety of planar substrates like silicon and glass. The irreversible bonding of such multi wafer stacks can be carried out using a brief exposure of both bonding surfaces prior to bonding to Oxygen plasma [21]. Soft lithography using PDMS offers several advantages like low cost of fabrication, rapid processing, reusability of the SU-8 master for multiple runs, facile sealing and bonding to a number of different substrates particularly in case of reversible bonding, and multilayer fabrication to create complex three-dimensional systems etc.. PDMS has good optical transparency from 230 nm onwards and covers the whole visible spectrum. Its elastomeric properties allow for easy interconnections between macro to microfluidic platforms and the properties are particularly helpful in realizing on-chip fluid handling components like valves, pumps, mixers, reactors, sensors etc. [22].

2.4 Micro-Scale Replication by Double Inversion (MRDI) Process

Biological and chemical applications require micro-fluidic devices with micro/nanoscale mechanical structures. Present fabrication techniques suffer from a low pattern transfer quality particularly if the feature sizes are in the nanoscale during the simultaneous embossing of the microscale and nanoscale patterns into a thermoplastic polymeric substrate since the polymer flow becomes insufficient. Fabrication of 3-D micro and nano-structures require expensive and time-consuming lithography assisted techniques and in some cases very high cost is involved in realizing these mechanical structures through the use of processes like electron or ion beam writing or nanolithography etc. [23]. In order to address the problems of lithography driven processes we have developed a low cost and high throughput replication based process called micro replication by double inversion (MRDI).

Figure 2.5 shows schematic of a standard replication process. The various steps involved in such a process are (a) pouring the liquid monomer onto the master (b) master and replica separation after photo-polymerisation by exposure to UV-light (c) The use of the replica (with some surface pre-treatment) as a new master for a further duplication of the features into another polymeric substrate. After polymerisation and separation the second replica contains the same structures as the initial one. (Represented in Fig. 2.5a–d). The master in MRDI process can also be made using laser micromachining as shown in Fig. 2.6.

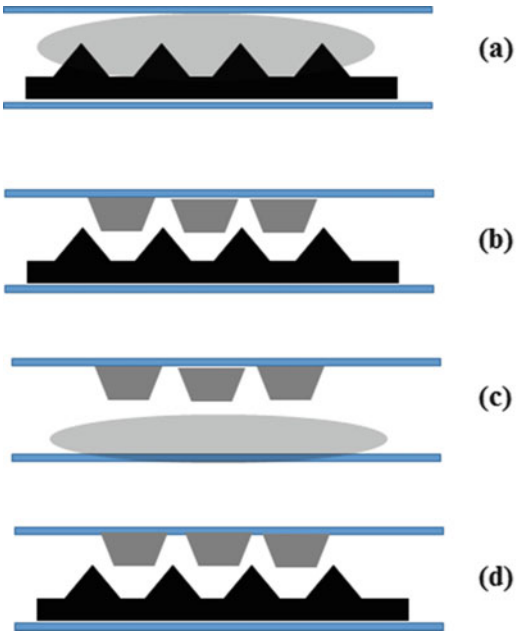

Fig. 2.5 Schematic representation of replication process

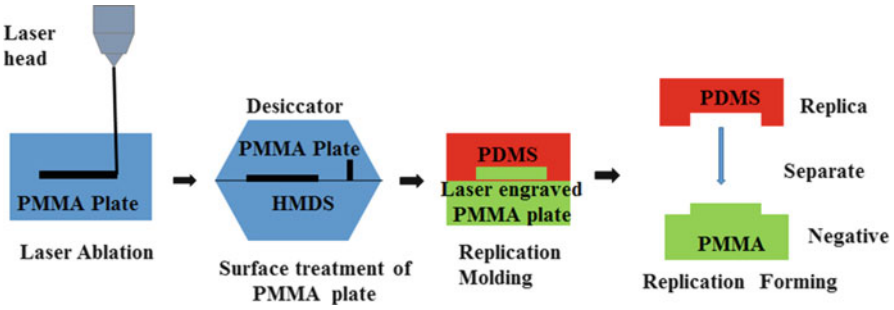

Fig. 2.6 Schematic representation of MRDI process

The principle advantages offered by the MRDI process are: (1) a sturdy mold, (2) repeated use of the mold for replication of polymer, (3) an overall inexpensive process as compared to other photolithography-driven processes,(4) A reusable mold, and (5) the use of laser ablation or other micromachining techniques for mold making.

PDMS replica mold is widely used for channel making in microfluidic applications although when we talk of embedded channels and features there are some very serious limitations of replication and moulding processes [24]. For example if the structure that is to be realized is a long micro-channel which is embedded within a chunk of the polymer PDMS both replication and moulding process done in the way as explained and also the MRDI may prove out to be failures and if done as a sandwiching between two replicated surface may impose limitations in terms of accurate alignment. In order to address these issues a replication and moulding technique has been developed with wires where the features and structures are replicated as embedded features within polymeric domains [25].

2.5 Embedded Structures with Replication and Moulding Processes

An easy fabrication procedure has been developed for three dimensional structures with soft materials like PDMS [26]. This has been used to develop micro-channel arrays within PDMS matrices which in a separate module as described below been tested for micro vibration control. An array of upto six rows of micro-channels with 20 numbers of micro-channels in each row have been fabricated using this procedure and in a very innovative manner The process was initiated with a micro drilling exercise wherein 200 μm diameter holes (20 in numbers) were drilled using MIKROTOOLS (DT 100, Singapore) machine tool in a simple plastic mold box using a CAD package on the side walls of this mold box. The centre to centre distance between these holes in x and y direction were taken as 2 mm. In order to

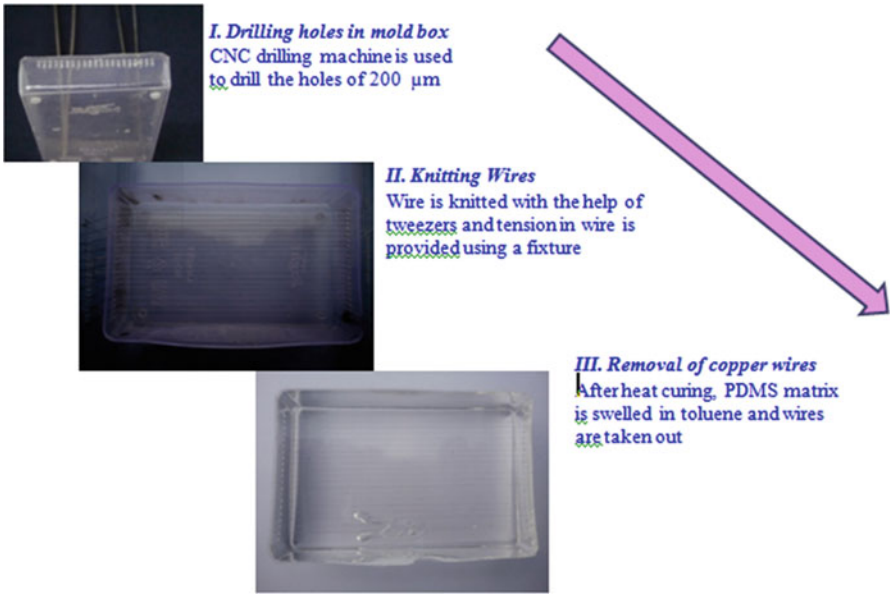

Fig. 2.7 Dimensional micro-channel arrays within PDMS blocks using thin circular copper wires. (Reproduced from Singh et al. [27] with permission from the Institute of Electrical and Electronics Engineers)

realize high aspect ratio micro-channels, thin wires of copper etched to a diameter of 50–80 µm were inserted between opposing holes in a mold box with a special tweezers and provided with finite tension using a special jig developed for this purpose. PDMS commercially available in a 10:1 ratio of a silicone rubber to curing agent was poured into the plastic box over the wires and replicated the wire array. This was followed by a release mechanism which comprised of a swelling step wherein the matrix with embedded wire array was taken out curing the PDMS and dipped in toluene for a finite amount of time. This swelling of PDMS matrix was performed mainly to release the grip over the embedded wires. This was followed by another shrinking step wherein the assembly was heat cured and the whole PDMS shrinks back to a smaller size. Figure 2.5 shows the process flow chart of this technique (Detailed in Fig. 2.7).

There has also been utilization of this wire based replication technique for the development of embedded fluid handling structures like microvalves etc. [28].

Figure 2.8 shows an embedded assembly of micro-valving as reported by Singh et al. In Fig. 2.8 there are two embedded channel in a piece of PDMS where the central channel shows a 80 µm channel and the solenoidal track around this central channel shows an embedded valve structure which can be inflated/deflated using compressed air so that it can squeeze the inner channel and act as a fluid valving device.

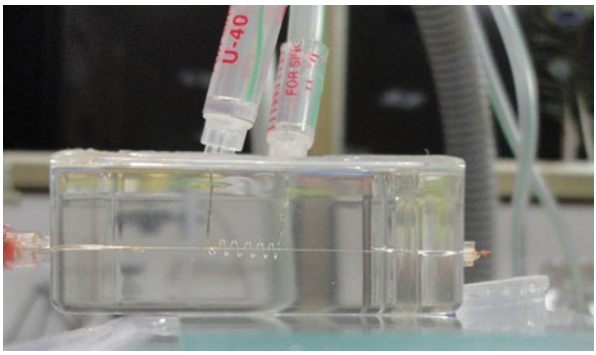

Fig. 2.8 Solenoid microvalve (Reproduced from Singh et al. [29] with permission from the Springer)

There are many other soft lithography approaches which have been reported in literature like solvent assisted micromoulding, nanoimprint lithography and dip pen lithography etc. Where the patterning is carried out at various scales with soft materials [30].

3 Microfluidics for Flow Control and Some Novel Effects

The early applications of microfluidic technologies have been mostly in chemical/biochemical analysis. The field of microfluidics offers numerous capabilities like rapid sensing and detection of analytes corresponding to limited concentration, rapidity of performance, easy usage with minimal human intervention, good resolution using very small quantity of sample volume and thus offering solutions to low cost diagnostics etc. Micro-flows are mostly laminar with values of Reynold's no. in the range of less than 1 and this laminarity is an advantage in some of the typical requirements of sensitive diagnostics like single cell isolation, single cell manipulation and detection, drug delivery etc. Microfluidics also offers possibilities to control concentration of sample in both space and time [1].

The laminar nature of Micro-flows makes molecular diffusion the only means to facilitate mixing in micro-scaled devices in the absence of convective transverse fluid motion. For a typical microscale device the diffusion length scale being large and the diffusion constant being very small for fluids ensures a very high diffusion time. This coupled with the laminar nature of microflows gives rise to a very interesting domain where various spatial and temporal strategies are utilized by various micro-chip designs to micro-scale actuation for enabling a reduced inter-diffusion length causing the flows to mix vigorously and sometimes in a controlled manner.

There has been a lot of research on micro-mixing methodologies, which focus primarily on increasing the contact surface between two streams for diffusion through multi-lamination strategies. The multi-lamination in flows can be achieved easily by stacking different streams in parallel, perpendicular, radial, as well as

angular orientations in respect of the flow direction. Various strategies have been developed for micro-mixing which has been broadly classified as Active and Passive mixing.

3.1 Micro-mixer Design and Characterization

A micro-mixer is a device which can passively (without using energy) or actively (with external energy) is enabled to mix multiple fluids. This device is associated heavily with key technological advancements in many fields like chemical engineering, pharmaceuticals, bio-chemistry, analytical chemistry and high-throughput synthesis and drug screening etc. The micro pathways or parts which are heavily deployed in promoting active or passive mixing may vary from a long serpentine channel to a piezoelectrically vibrating membrane.

The development of micro-mixers has progressed rapidly in the last decade. Initially, the devices manufactured used to be housed within silicon or glass wafers [31] and from then a number of micro-mixers with polymeric parts have been fabricated and successfully developed [32]. As a result of their overall simple design, passive micromixers have found a lot of applications as analytical chemistry tools. While surveying the various the polymeric microfluidic systems, a simply designed microfluidic system with efficient passive micromixing is a natural choice for many applications in chemical and biochemical analyses [33]. Researchers have proposed various designs of micro-mixers (Fig. 2.9) and their use including simple

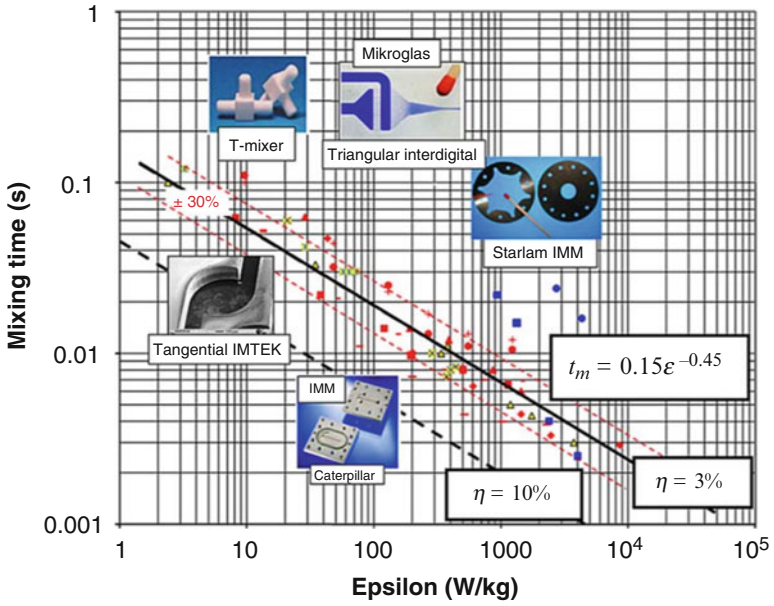

Fig. 2.9 Comparison of various micromixers with respect to time and specific power dissipation (Reproduced from Falk and Commenge [34] with permission from the Elsevier)

T-type or Y-type micromixers and also parallel and sequential Lamination mixer [34].

Nanoparticle synthesis using microscale controlled mixing is a new essence that is being carried out in micromixers and microreactors. The nanoparticles so synthesized have a much skewed distribution and can be custom-made in regards to the average size of the distribution and also the standard deviation on the particle diameters [35].

Many materials which are either amenable to microfabrication such as Silicon and glass or to laser micromachining such as PDMS and PMMA as discussed in previous sections can be employed for the fabrication of the flow channels which constitute the path in a micromixer. Sometimes when the requirement of fabrication is extremely complex precision orientated techniques like micro-stereolithography [36], two photon processes [37] etc. are deployed to realized complex 3-D flow paths.

3.2 *Bilayer Staggered Herringbone Micromixers (BSHM)*

A novel modification of passive micro-mixers has been attempted by Choudhary et al. [38] wherein a method is developed to fabricate micro fluidic devices using MRDI technique as described above onto soft polymeric material PDMS [38]. It has been observed that the novel fabrication method—MRDI was able to produce excellent replication results. The limitation that the process faced however came from the lack of control on speed and power in the laser ablation step which had to be iterated with design of experiments (DOE) strategy. The dimensions used for fabrication were simulated and arrived at in this work (channel width = 100 μm; channel depth = 100 μm; herringbone = 30 μm deep and 50 μm wide). Well shaped herringbone structures were created on the path of flow and mixing was thoroughly evaluated as a function of the overlapping herringbones arm. It was found that as the overall ratio of the herringbone arms on the top and bottom sides of the flow path was reduced the flow length reduced. The image of fabricated herringbone micromixer has been shown in Fig. 2.10a, b and a snap shot of the experimental mixing data evaluated through dilution of a fluorescence marker dye is provide in Fig. 2.10c.

3.3 *Long Microchannel Arrays as Vibration Pads*

Long microchannels arrays have been also found to be suitable for custom made vibration damping characteristics and can passively reduce mechanical vibrations at a range of low frequencies and as such can be used for passive micro-vibration

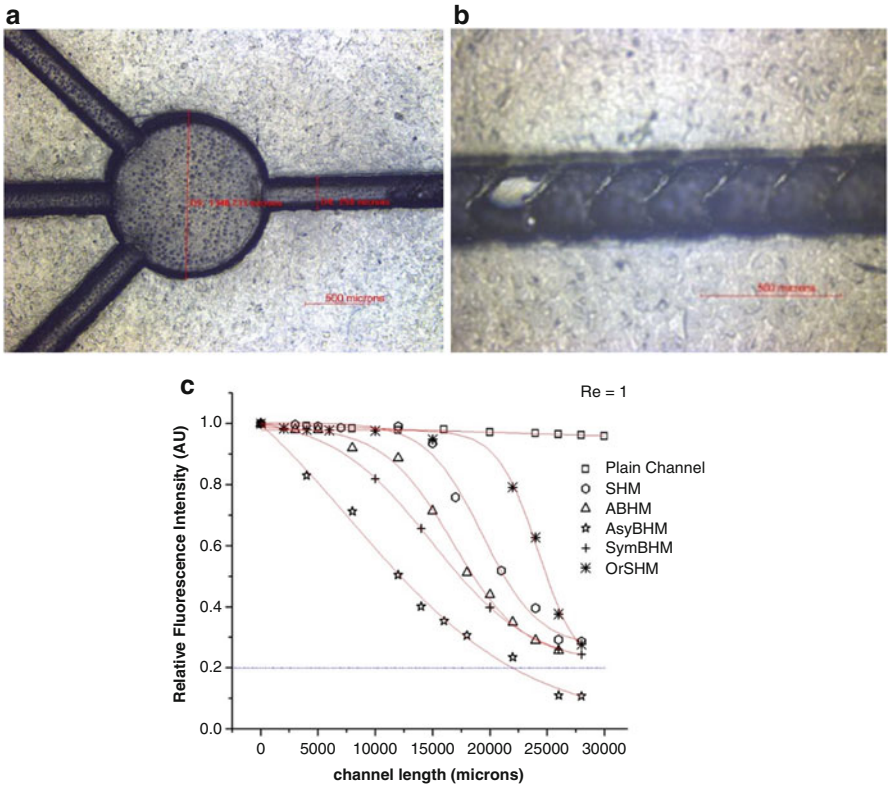

Fig. 2.10 PDMS Replica obtained after soft lithography and herringbone structures ((**a**), (**b**)); (**c**) Mixing performance by dilution of a fluorescence dye in a plain channel, symmetric Herringbone structure, alternate bilayer Herringbone mixer, Asymmetric bilayer herringbone mixer, symmetric bilayer herringbone mixer and oblique ridges and staggered herringbone mixer (Reproduced from Choudhary et al. [27] with permission from the Springer)

damping. The channel array is embedded in blocks of viscoelastic materials in an oil filled and hermetically sealed manner [27]. In this work, the passive response of a replicated array of oil-filled micro-channels, structured within a block of PDMS is reported. Constrained and unconstrained vibration-damping experiments are performed on this block, by applying an excitation signal transversely at the geometric centre of the lower face of the block; its vibration suppression ability is detected. Figure 2.11 shows the constrained and unconstrained configurations schematically and the respective loss factor data with no. of embedded channel layers.

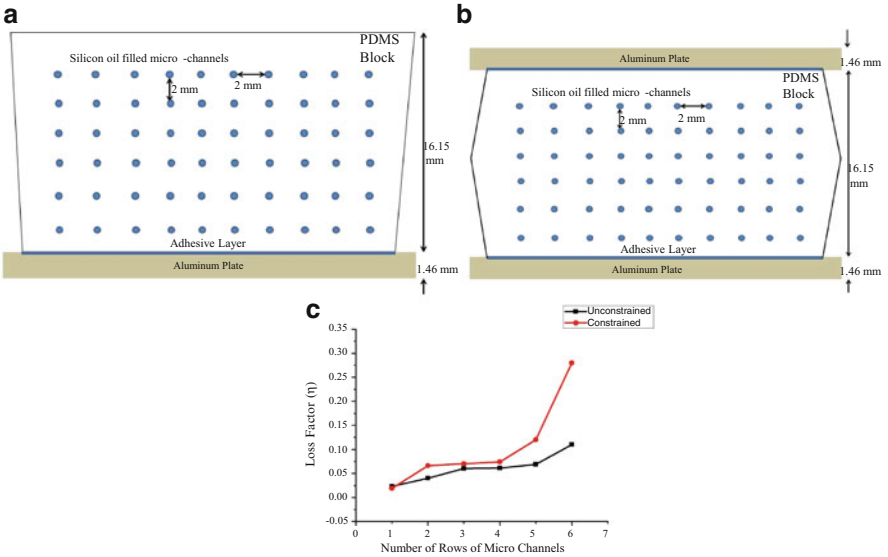

Fig. 2.11 (**a**) Schematic of unconstrained mode damping. (**b**) Schematic of constrained mode damping. (**c**) Loss factor plot with respect to number of rows of embedded channels in both constrained and unconstrained damping analysis (Reproduced from Singh et al. [27] with permission from the Institute of Electrical and Electronics Engineers)

3.4 Micro-pump

Micro-pump are MEMS based fluid handling devices which again work passively or actively to initiate flow through micro-channels. One of their critical purposes is to initiate micro-flows of samples of fluids (either chemical or biochemical) for reaction assays for diagnostics applications. The pump volume is generally of the order of volume of the sample that is being transported. Micro-pumps can be of mechanical or non-mechanical type depending on the actuation principle that they may possess. In mechanical micro-pumps the actuation methods can be electrostatic, magnetic, piezoelectric, pneumatic and thermo-pneumatic etc. while in non-mechanical systems actuation scheme like electro-osmotic, electro-hydrodynamic, electrochemical or ultrasonic etc. can be deployed. It is generally observed that the flow rates in case of mechanical micro-pumps are orders of magnitude more than the non-mechanical micro-pumps.

The first ever peristaltic micro-pump was patented by Smits in 1989. This was a silicon based device fabricated using already established MEMS fabrication technology, and was provided with a set of piezoelectric valves which would deflect and squeeze out on chambers in a sequential manner. This pump had a maximum flow rate of 3 μL/min at zero back pressure and a Maximum Pressure head of 0.6 m H_2O. Further, it was observed that the discharge rate varied linearly with the back pressure till a threshold frequency of 15 Hz was met beyond which it started to fall

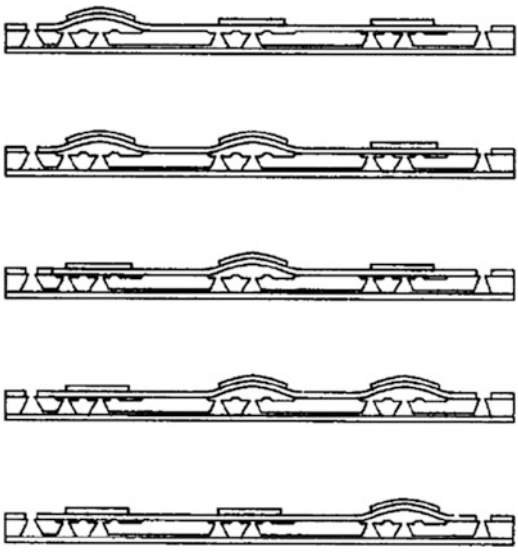

Fig. 2.12 Pumping sequence of the peristaltic pump (Reproduced from Smits [38] with permission from the Elsevier)

off. At frequencies more or equal to 50 Hz, no pumping action was observed which was attributed to viscosity of the pumped fluid. In another work reported later [39], the same group reported an improvised version of micro-pump capable of delivering 100 μL/min at zero back pressure as shown in Fig. 2.12.

Peristalsis with soft polymeric membranes have served the purpose of achieving micro flows although literature has only thoroughly looked at their performance metrics like flow rate [40], ability to withstand back pressure [41], actuation mechanism [42, 43] and fabrication strategies. The most widely used discreet peristaltic strategy that is worth mentioning in this context [44] uses two replicated and molded layers of Poly-dimethylsiloxane (PDMS) bonded over a hard substrate with the top layer being used as the actuator layer wherein controlled compressed air is used to pinch circular chambers inter-connected by thin replicated channels in the second layer. Some earlier reports on micro-pumps as reported by Kant et al. [45] involves such architectures as described in the next section.

3.4.1 Micro-pumping System with Peristaltic Motion

Kant et al. have provided an innovative design of peristalsis based micro pump with an optimized fluid chambers possessing enhanced discharge efficiency per unit volume of the pumping architecture and reduced reverse flow, very often important from the standpoint of blood cell sorting assays, within the pumping chamber where full delivery of fluid containment is critical. Researchers have given a simulation on COMSOL to optimize the chamber design to evaluate the effect of actuator membrane interaction. Optimized geometrical profile formulated above was seen to allow the maximum contact area between fluid containment and actuating

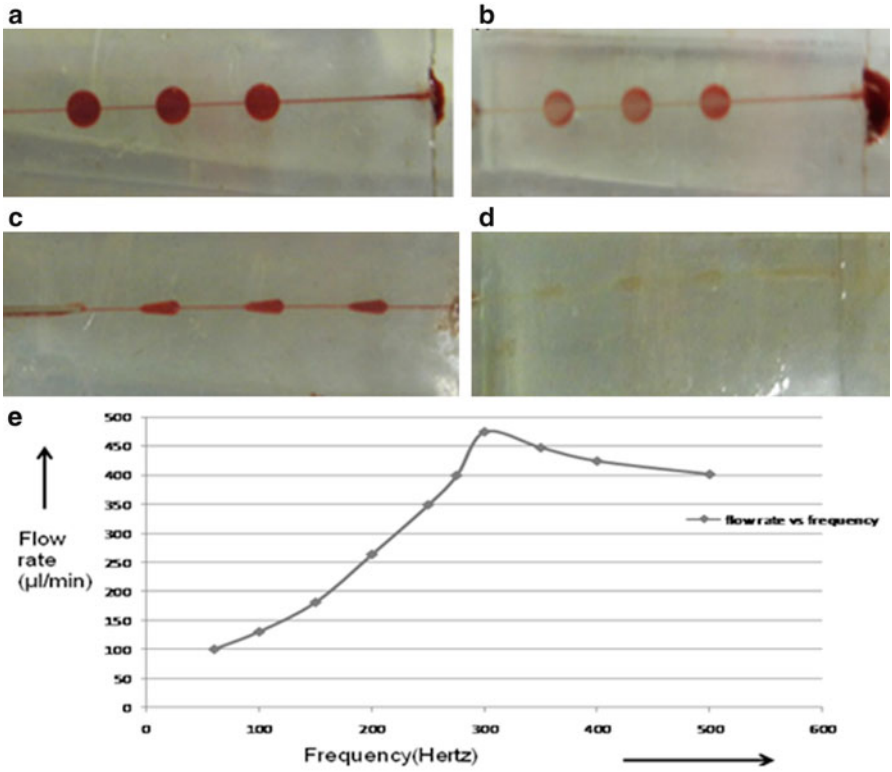

Fig. 2.13 (**a**) Optical micrograph of pumping chambers in the circular design case before start of wash cycle (**b**) at the end of wash cycle (**c**) optical micrograph of pumping chambers in the optimized design case before start of wash cycle (**d**) at the end of wash cycle (**e**) Discharge with respect to operating frequency of the modified design as in case (**c**) (Reproduced from Kant et al. [45] with permission from the Springer)

membrane thus reducing the problem of fluid retainability inside the chambers. Figure 2.13 shows optical micrograph of pumping chamber for both type of design before and after the wash cycle and the discharge performance of the modified chamber design as in part (c) and (d). Additionally Fig. 2.13e shows the discharge related to (c) configuration.

New design of pumping system (experimentally) decreases the percentage retainability of biological and other fluids contained within the chambers which make it a comparatively high efficiency micro-pumping system as compared to conventional design with circular membrane and chambers.

3.5 *Micro-valve*

Micro-valves are designed to control the switching action of flows in microchannels. This helps in controlling the flow rates so that proper manipulation of the biological entities being carried by biological fluids can occur and hence the overall efficiency of the microfluidic system to handle and deliver increases. Micro-valves can also be characterized as active and passive microvales. Atwe et al. has developed a novel pH-sensitive hydrogel based micro-valve for intelligent valving system for metered flow [46]. Figure 2.14a shows the design of micro-valve using hydrogel developed through precursors chitosan and polyvinyl alcohol (PVA).

The hydrogel solution has been shown to be prepared through Chitosan and polyvinyl alcohol (PVA) in acetic acid (CH_3COOH) and crystallized using glutaraldehyde, crosslinking agent in thin wafers form and this has been found to be very sensitive to pH changes. The pore structure of hydrogel had been investigated

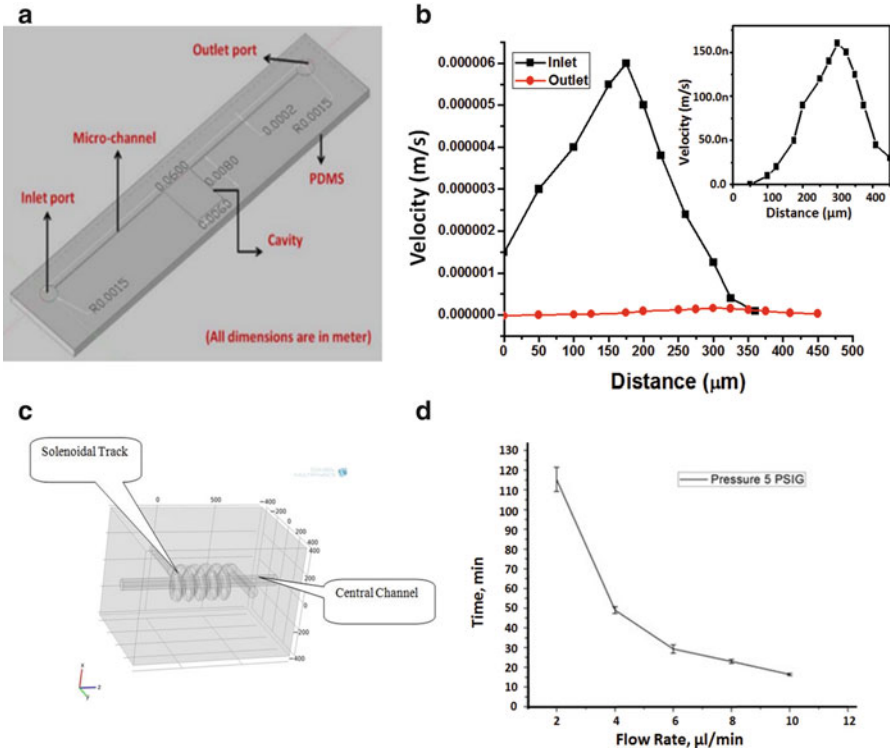

Fig. 2.14 (**a**) Design of the micro-valve; (**b**) Valve performance through PIV measurements as a function of diametral distance from wall of the channel; (**c**) architecture of a solenoidal microvalve; (**d**) valve performance plot of flow rate versus time corresponding to a compressed air pressure of 5 psi. (Reproduced from Atwe et al. [46] and Singh et al. [47] with permission from the Springer)

through Field Emission Scanning Electron Microscopy (FESEM) and thin wafers of the gel were physically placed inside PDMS microchannels which blocked the main flow as the pH in the actuating channels changed suitably. Flow metering in channels was observed till complete realized of valving. This device was further precisely characterized with micro PIV using a solution containing fluorescent polymeric micro beads. The principle advantage device is the small range of pH (3–7) over which the valving response was observed.

Singh et al. [29] has reported a pneumatically actuated solenoid micro-valve design with performance evaluation in terms of flow constriction. Figure 2.8 reported earlier has already shown a schematic of this valve. The valve performance has been evaluated with particle image velocimetry (PIV) (see Fig. 2.14b–d) [29]. These valves are definitely an advantage over quake valves which were done using two layers of microstructured PDMS with the bottom layer containing the micro-channels as very thin and the top layer containing the valve structured at the bottom of the top layer. These valves have so miniscule response time that they almost close immediately qualifying them to be digital in nature. Design modification has been performed in these digital valves to solve the leakage/leaching problem, with a completely different synthesis process, wherein the closing arrangement of a Quake valve has been varied from top down to radially inwards across the whole cross-section of the micro-channel. The valve's design enables its wide applicability to microfluidics in drug delivery; study the flow of body fluids across vasculature like flow within embedded channels etc.

4 Micro-cantilevers for Mass Based Sensing and Diagnostics

Micro-cantilever is a beam fixed or anchored at only one end. The beam carries load to the support where it is forced against by a moment and shear load. A micro-cantilever is a device that can act as a sensor may be biosensor or gas sensor else for various other applications by detecting changes in cantilever bending through optical deflection method or piezoresistive method or vibrational frequency method. The cantilever bending occurs when a specific mass of analyte or biomolecule is adsorbed on the surface of the cantilever and leads to a change in the surface energy of this thin cantilever structure. Miniaturisation of cantilever helps sensing the presence of trace elements in chemical and biological analytes as well as small mechanical displacement etc. Fabrication of micro-cantilevers is a multiple step lithography driven process where the cantilever structure is first realized using surface micromachining and this is succeeded by bulk micromachining to release the cantilever structure additively built in the first step. The fabrication of cantilever micro-structures can be done using different materials like silicon, silicon dioxide, aluminium, gold and of different polymers.

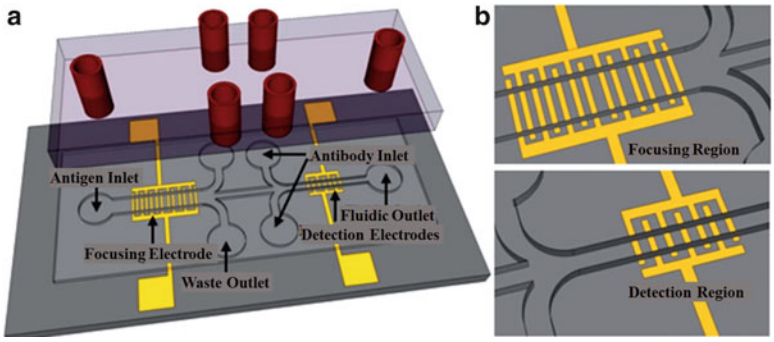

Fig. 2.15 Three dimensional schematic of (**a**) impedance based biosensor for pathogen detection. (**b**) Magnified view of the focusing region and detection region (Reproduced from Ghoshdastidar et al. [48] with permission from the Royal Society of Chemistry)

Both micro-cantilevers as well as other three-dimensional micro-structures have been exclusively used for sensing and diagnostics. Ghoshdastidar et al. [48] have made micro-machined impedance bio-sensor for accurate and rapid detection of E. coli through interdigited electrode structures. They have fabricated two sets of interdigitated electrodes made of gold, embedded in a SU-8/PDMS micro-channels. Using dielectrophoretic trapping the microorganism E. coli was focused on the centre of the microchannel where a second set of electrodes were used to sense through impedance spectroscopy the type and the concentration of the micro-organism. Figure 2.15 shows the three dimensional schematic of biosensor platform.

Boehm et al. [49] introduced a methodology for fast detection of bacteria through a micro-fluidic lab-on-chip device to detect cells using antibody immobilization. Composite self-excited PZT-Cantilever was fabricated and their frequency of resonance was measured both in water and air. Resonant frequency of the second mode was observed to decrease due to pathogen attachment by Campbell et al. [50]. Weeks et al. [51] have reported detection of Salmonella strains using silicon nitride based micro-cantilever. V shaped cantilevers were used which were 180 mm long and 18 mm wide. The cantilever was functionalized using antibody S. Heidb. The cantilever deflection with respect to the Salmonella concentration cfu/ml was obtained and it was directly observed that with the increase in concentration of the sample, deflection was increased. Initially S. Typh strains were injected at 100 cfu/mL but no deflections were noticed but as the S. Heidb strains were injected deflections were obtained within 20 s.

Ilic et al. [52] have done virus detection using nanoelectromechanical devices using a non-pathogenic insect baculovirus to test the ability to specifically bind and detect small number of virus particles. Arrays of surface, antibody-coated polycrystalline silicon nanomechanical free standing cantilever beams were used to detect the binding from varying amounts of concentrations of baculo viruses in a buffer solution. Figure 2.16 shows the fabrication technique and SEM image of the fabricated micro-cantilever. Because of their small mass, the 0.5 mm $\times$ 36 mm

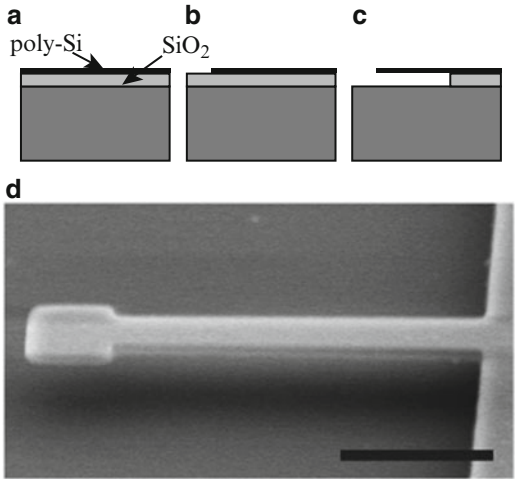

Fig. 2.16 Fabrication sequence of the nanomechanical oscillators; (**a**) Thermal oxidation and LPCVD deposition of the polycrystalline silicon device layer; (**b**) Lithographic definition of the oscillator; (**c**) Sacrificial silicon dioxide removal using HF; (d) Free standing cantilever (L = 6 μm, w = 0.5 μm, t = 150 nm) SEM image (Reproduced from Ilic et al. [52] with permission from the American Institute of Physics)

cantilevers have good amount of mass sensitivities of the order of 10 – 19 g/Hz, enabling the detection of an immobilized AcV1 antibody monolayer corresponding to a mass of about 3×10^{-15} g. Reviewing some of the papers it can be observed that cantilevers deflect in the range of 10^5–10^6 cfu/mL of micro-organisms. Thus although these numbers are not good with respect to PCR methods which can go up to sensitivities of few tens of cells but still from a rapidity point of view these test may serve to be better.

Secondly there may be problems during frequency shifts which can be found by the work reported by Ilic et al. [53] while detecting the E. Coli due to low quality factor of the cantilever structure in liquid and also the relative position of the immobilized microbe along the cantilever from its tip end. Figure 2.17 shows the frequency shift while capturing E. coli cells on cantilever surfaces.

Our research group has also started fabrication of micro-cantilever structures with thin films which are of significant importance in biosensing applications. Fabrication of thin film micro-cantilever possesses major difficulties like releasing the structures and etchants selectivity. One of the most important problem is stiction problem which occurs during wet etching. Releasing the cantilever without using any sacrificial layer has been demonstrated by our work [54]. Other than that Shipley photoresist S-1813 when hard baked, can act as a good protective layer from etchants. Several films of aluminium (Al) of thicknesses ranging between 200 and 800 nm have been deposited on cleaned Si-wafers through sputtering process. On the top surface of this Al thin film cantilever structures were patterned through positive photoresist S-1813 (M/s Shipley). The positive photoresist structure acted as a mask or protective layer for the TMAH etching process that was used subsequently for releasing of the cantilever structures. The Al thin film was first etched off through the vias opened up for the remaining portion of the film for the top elevation of the mask drawing. The etching of the aluminium from the opened positions were further carried out using Transene solution at a temperature of 50 °C.

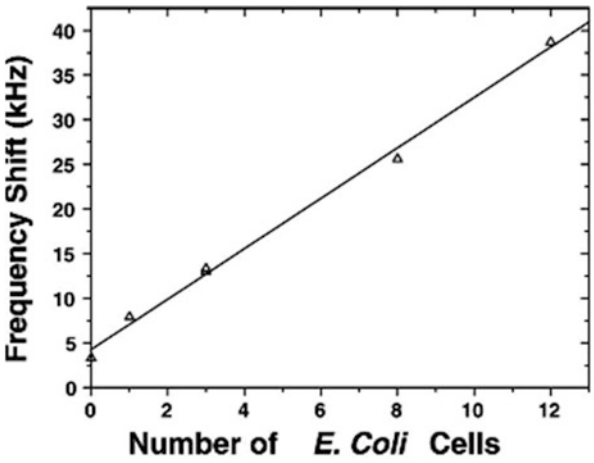

Fig. 2.17 Frequency shift observed with increase in number of E. coli cells (Reproduced from Ilic et al. [53] with permission from the American Institute of Physics)

For releasing the Al micro-cantilever a second step of masking and anisotropic wet etching was done with TMAH etchant [55]. Figure 2.18a shows a detailed fabrication flowchart of the process used for etching of silicon cantilevers. Figure 2.18b shows the FESEM image of a thin film and Fig. 2.18c shows a force deflection characterization using a nano-indenter. Our studies have revealed a very high resilience (almost equal to that of natural rubber) of these metallic cantilever structures [56].

Our group has also been heavily involved in fabrication of polymeric cantilevers using the photosensitive epoxy based polymer SU-8. These SU8 cantilevers have been developed using a one-step lithography based process using maskless gray-scale lithography (MGL). Generally in photolithographic process there are only two states '0' or '1' i.e., the photoresist either stays or gets dissolved after exposure or during development but in gray-scale lithography a selective exposure process is possible by changing the gray-scale values. Also variation in exposure dose varies according to the penetration depth as offered by the photoresist to the laser beam.

In this work, we have tried to develop a methodology for fabricating three dimensional interdigitated micro cantilever structures of SU-8 through grayscale lithography. The difference in our cantilever is in terms of sectional thickness which has been realized at smallest level of 2 μm. Earlier researchers have shown a total thickness of 45 μm using different grades of SU-8. Our fabrication technique enables to fabricate at 1/20th the dimension achieved by earlier researchers. Thin cantilevers find a lot of prominence in the area of sensitive detection of biological entities. Figure 2.19 shows the FESEM image of fully dimensioned interdigitated micro cantilever structures. The hanging SU-8 structures are metallized and serve as interdigitated electrodes which may be able to capture and position single cells using dielectrophoresis process. The miniaturized nature of our architecture enables us to perform our studies on bacterial cells providing an opportunity to carry out stiffness based segregation cells.

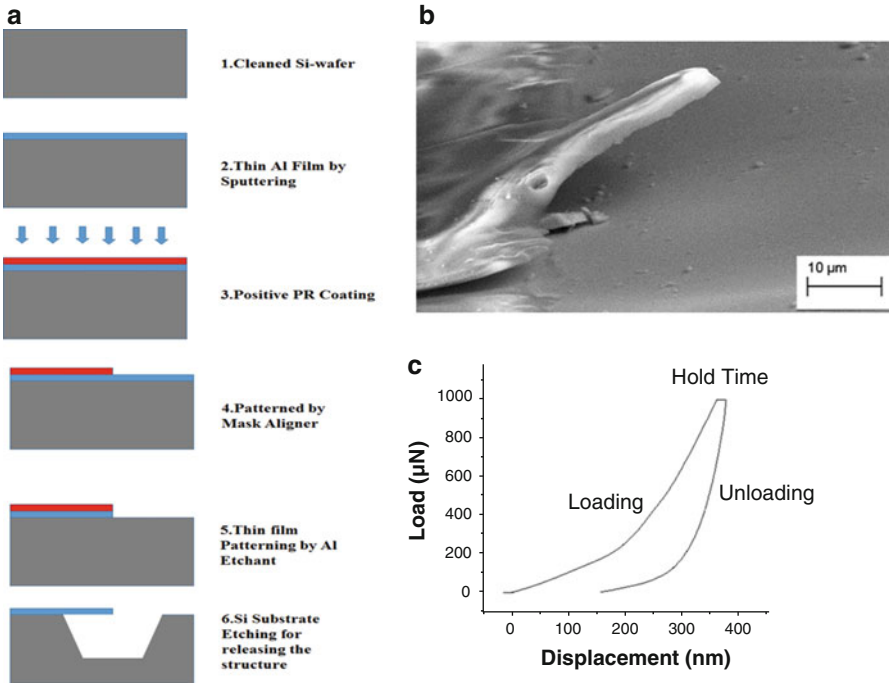

Fig. 2.18 (**a**) Fabrication flow chart for the process used (**b**) FESEM image of Al microcantilever 78 µm long and 28 µm width (**c**) Force displacement characterization on a nanoindenter

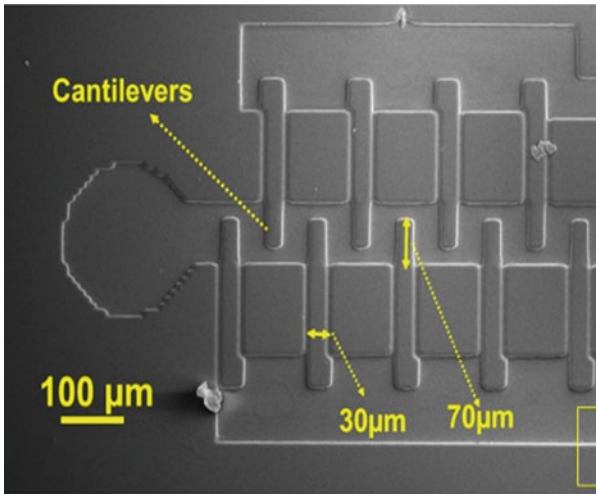

Fig. 2.19 Interdigitated cantilevers placed in microfluidic channel

5 Applications in Clinical Diagnostics

Using the basic principles and tools of microfluidics, various diagnostic applications are realized. These applications are focused on separation, modification, combination, replication of biological entities that would result in a signal transduction which may further be able to get detected with instrumentation or normal eyes. Applications range in many domains like paper microfluidics, PCR microchips, electrophoresis microchips, Gene delivery modules etc.

5.1 Paper Microfluidics: Applications in Clinical Diagnostics

Lateral flow technology is well suited for point-of-care disease diagnostics because it allows complex bio/chemical processing to be performed without the need for external instrumentation. It fulfils the criterion of world health organization (WHO) i.e., ASSURED (affordable, sensitive, specific, user-friendly, rapid and robust, equipment-free, and deliverable to users). Since the fabrication cost of paper based device is very less as compared to the equipment used towards bio-diagnostics like PCR and ELISA readers thus this technique is more affordable to a wide section of people who cannot afford expensive healthcare particularly in developing countries. There are several other advantages of using paper based diagnostic devices such as thin and easy to transport, lightweight, disposability, chemical modifiability and bio-compatibility [57]. Paper based devices can be fabricated using various methods such as photolithography [58], plotting with an analogue plotter [59], ink jet etching, plasma treatment [60], paper cutting, wax printing [61], ink jet printing [62], flexography [63], screen printing, laser treatment etc. [64].

The lateral flow tests often rely on antigen–antibody interactions to detect targets of interest in bodily fluids, such as serum, blood, or urine. Depending on the assay format, either the antigen or antibody is immobilized on the paper substrate as the capture agent. The targets of interest bind to the immobilized capture agent, resulting in visually distinguishable lines or spots generated by colorimetric, fluorescent, or enzymatic conjugates [65]. When conjugated gold/silver nanoparticles-antibodies bind to specific biomarkers thus changing the overall size of the nanoparticle assembly and thus their absorption properties which results in a colorimetric assay. The change in colour can be even detectable through a commercial smart phone camera [66].

The basic design of a lateral-flow test strip, shown in Fig. 2.20, comprises four porous pads. The sample pad, conjugate pad and absorbent pad are usually made by filter paper. While the test line and control line is made on nitrocellulose membrane. The nitrocellulose membrane is a microporous structure which is made from the nitrocellulose and nonwoven materials (glass, fiber or cellulose etc.). The nitrocellulose membrane is preferred as a substrate for the formation of biochemical

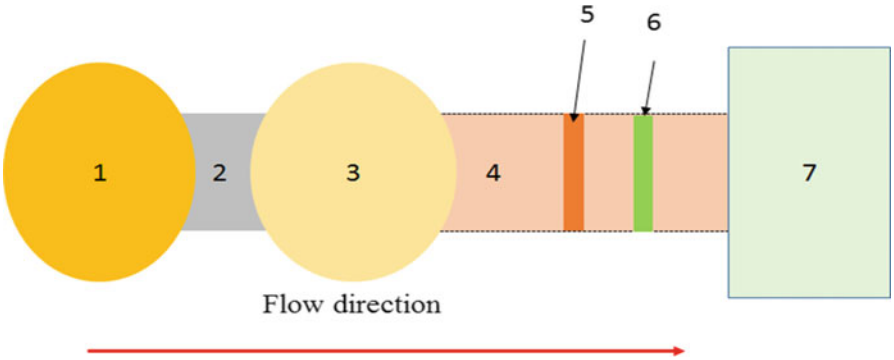

Fig. 2.20 The schematic diagram of paper based colorimetric detection assay. (1) Sample pad: blood sample with viral proteins pipetted onto it; (2) filter paper: through which blood is migrated towards conjugated pad; (3) conjugated pad: conjugated antibody-nano nanoparticles pipetted onto it; (4) nitrocellulose membrane (5) test line: visualization of color change if there is any positive test result. (6) Control area (7) absorbent pad: to wick the extra fluid

complexes because of the various reasons; First, high rate of adsorption of the protein on it. Second, chemistries that make the membrane wettable with aqueous solution which helps in protein adsorption. Third, the pore size of membrane can be controlled according to requirement. The general detection steps of paper assay is depicted in Fig. 2.20.

In the past decade, lateral flow or paper based assay have been widely used in various types of biologically relevant applications including paper-based molecular assays, paper-based ELISA (P-ELISA), paper-based nucleic acid assays, and paper-based cell assays for rapid diagnostic of protozoan and viral diseases like malaria, dengue etc. [57]. Compare to other existing detection techniques, the Paper based rapid diagnostic kits (RDT) require little or no pre sample preparation and give results in few minutes. Guidelines for the evaluation of malaria diagnostic assays have been published and provide a standardized approach to diagnostic assessment [67]. In recent years various researchers has performed testing of Plasmodium falciparum on paper based device. Pereira et al. [68] fabricated the 3-D paper based device to detect malaria biomarker in a single step. The concentration and detection steps were integrated into single step that occurs entirely within a portable paper-based diagnostic strip. Figure 2.21 shows the schematic device for malaria detection on a single chip.

Weaver et al. [69] performed chemical colour tests embedded on a paper card which can significantly identify formulations corresponding to very low quality anti-malarial drugs. The presence or absence of chloroquine (CQ), doxycycline (DOX), quinine, sulfadoxine, pyrimethamine, and primaquine antimalarial medications, were examined. The sensitivity of the developed test card varies from 90 to 100 % with no false positives in the absence of pharmaceutical. For detection of extremely low concentrations of parasite target, a combined system has been developed which combines the isothermal amplification (Recombinase Polymerase

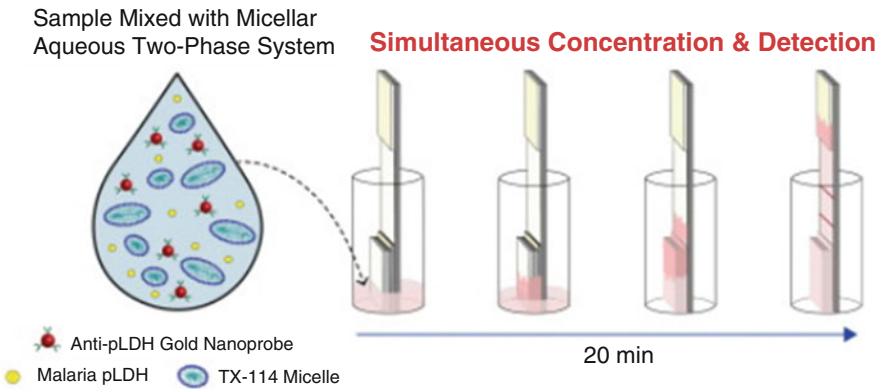

Fig. 2.21 Schematic diagram of paper based device for malaria detection in a single step (Reproduced from Pereira et al. [68] with permission from the Elsevier)

Amplification) and colorimetric detection of a malaria DNA sequence [70]. Paper based micro-fluidic device has also been used in detection of uric acid, glucose using gold nanoparticles [71].

Dengue viral has been diagnosed using the conventional techniques like PCR (polymerase chain reaction) and ELISA (enzyme-linked immunosorbent assay) [72], even these methods are highly accurate but they need a highly clean lab and expert people to perform the test. In the developing countries like, India where the lab facilities are not appropriate in all the locations especially in rural areas, the paper based detection can play a complementary role. Yen et al. [73] developed a paper based testing device which can give a patient a diagnosis within few minutes on whether they have dengue, Ebola or yellow fevers. The red, green and orange silver nanoparticles were immobilized to the respective antibodies that bind the spiked proteins. These antibodies were then attached to a small piece of paper. Instead of whole blood samples, salivary fluid has also been used for dengue detection because it is an important source of biomarkers and is useful for rapid point-of-care diagnostics. Salivary fluids carries the immunoglobulins (e.g., IgGs and IgMs), lymphocytes and plasma cells, which may serve as biomarker in point of care diagnostics. But major limitation of salivary fluid as a sample is that it cannot be applied directly to commercially available lateral flow test strips because it causes the non-specifically binding of conjugated particles to the nitrocellulose membrane. To overcome this problem, Yi et al. [65] recently developed a rapid test for the detection of anti-DENV IgG in saliva. They introduced samples and reagent in separate flow paths. The sample flowed through a matrix of fiber glass which reduces the non-specific adhesion caused by the salivary substances. Figure 2.22 shows the design of device for dengue detection.

The device gave good results in saliva samples spiked with IgG but requires further improvement to detect IgG extracted directly from the blood of dengue-infected patients. To improve the sensitivity (It is the ability of a paper based assay test to correctly recognize patients who have a given disease or disorder.) and

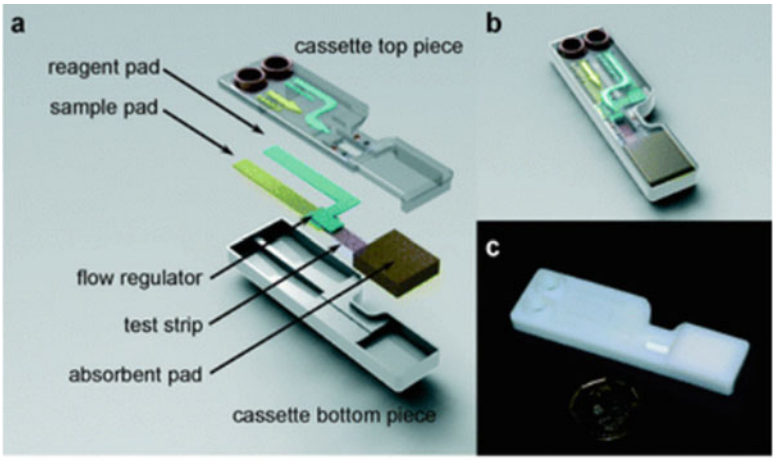

Fig. 2.22 Device for the stacking lateral flow immunoassay; (**a**) The exploded view of the device. The test assembly consists of a sample pad, a reagent pad, a flow regulator, a test strip and an absorbent pad. The test assembly is housed in the cassette; (**b**) The assembled stacking flow device; (**c**) Photograph of the stacking flow device prototyped with a 3D printer (Reproduced from Yi et al. [74] with permission from the Royal Society of Chemistry)

specificity (It is the ability of a paper based assay test to correctly exclude the healthy individuals) of the dengue detection, a methodology has been developed which combines reverse transcription loop-mediated isothermal amplification (RT-LAMP), paper based device and fluorescence based colorimetric detection [74].

5.1.1 Basic Principles of Fluid Flow in Paper Micro-fluidics

The flow through the paper occurs due to capillary action. The capillary action is governed by three main variables i.e., cohesive force, surface tension and adhesive force (Fig. 2.23). Capillary action happens only when the adhesive force is greater than cohesive force. When liquid is brought into contact with a dry paper, it will start absorbing liquid because there is an unbalanced pressure difference within the bulk phases [75]. The fluid can rise against gravity and it stops when the hydrostatic pressure balances the interfacial pressure difference.

Let us consider capillary rise in a cylindrical tube of inner radius r.

The equilibrium height h of the liquid within a capillary is obtained by

$$\Delta p = \frac{2\gamma_{LV}\cos\theta}{r} \tag{2.1}$$

The hydrostatic pressure is given as:

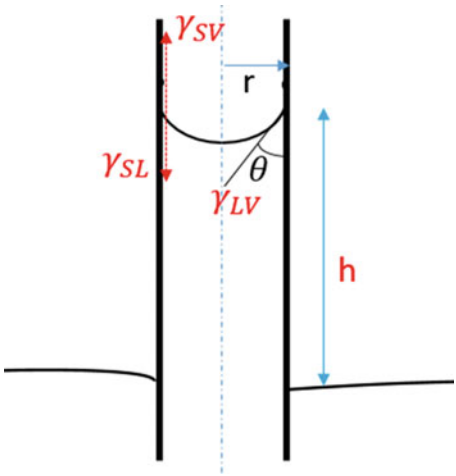

Fig. 2.23 Capillary rise in the tube

$$\Delta p = (\rho - \rho_v) g h \approx \rho g h \tag{2.2}$$

From (2.1) and (2.2):

$$\Rightarrow h = \frac{2\gamma_{LV}\cos\theta}{r\rho g} \tag{2.3}$$

Where γ_{LV} = interfacial surface tension of the liquid–vapor, γ_{SV} = interfacial surface tension between solid-vapor, γ_{SL} = interfacial surface tension between solid–liquid, ρ & ρ_v are the densities of liquid and the vapor and θ is the contact angle.

The transport of fluid on paper channel in 1-D can be estimated using the Lucas–Washburn equation [76]:

$$L = \sqrt{\frac{\gamma_{LV} D t \cos\theta}{4\mu}} \tag{2.4}$$

Where L is the distance moved by the fluid front, t is time, D is the average pore diameter, γ_{LV} is the surface tension, and μ is viscosity.

The above formula is useful in designing of paper channel. The length of paper channel is directly proportional to the square root of time. The volumetric flow rate (Q) of the fluid in a paper channel of constant width can be described by the Darcy's law:

$$Q = \frac{-kA}{\mu L}\Delta P \tag{2.5}$$

Where k is the permeability of the paper to the fluid, μ is the viscosity of the fluid, A is the cross sectional area of the channel perpendicular to flow, and ΔP is the pressure difference along the direction of flow over the length L [77]. Apart from the above governing equations the delivery of fluid depends on various other parameters such as properties of the porous materials, including pore size, pore structure and surface treatments etc.

Although these paper micro-fluidic point-of-care devices are capable of rapid detection at a lower price they are easy to use and eco-friendly. These devices have some limitations like the sample virus gets embedded in the pores of the paper device due to which only a small portion of the conjugated antibody-antigen reaches the test line resulting in an overall reduction of sensitivity etc. [78].

5.2 Electrophoresis

Electrophoresis is the process in which particles dispersed in the fluid move under the effect of uniform electric field. It was observed by Ferdinand Frederic Reuss in 1807. This effect comes under play due to the presence of charge interface between the particle surface and fluid around it. Electrophoresis helps in separating the molecules according to their size (smaller molecules travel with higher speed). Electrophoresis basically deals with applying a electric field on a particle and with respect to the charge present in the molecule, the molecule starts moving towards the oppositely charged electrode. Hence on this basis, electrophoresis can be divided in two types, one is cataphoresis (electrophoresis of positively charge ions) and other is anaphoresis (electrophoresis of negatively charged ions).

Figure 2.24 shows the effect of uniform electric field on the positively charge ion as well as on the neutral body. The positively charged ion starts moving towards the negative pole while the neutral body experiences no external force.

Electrophoresis can be done using three techniques namely:

1. Gel Electrophoresis
2. Capillary Electrophoresis
3. Surface Electrophoresis

(a) **Gel Electrophoresis**

Gel Electrophoresis is the technique used in electrophoresis to separate the molecules depending on their size using a porous matrix. While using this porous matrix, which is generally made up of agarose gel, an electric field is passed making one side of the matrix positive and opposite size of the matrix as negative. In this manner when we keep our negative charges on the side of the negative pole, and start the field, it will quickly start moving to the positive terminal through the gel matrix. Agarose is the polysaccharide polymer material. When the solution of this is made, it makes a porous kind of structure with very small size pores, which are just enough to allow molecules like DNA/RNA to pass. When the field is applied, the smaller molecules start

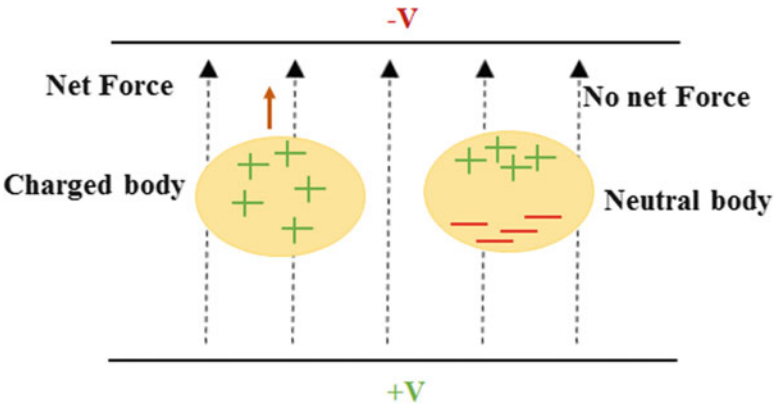

Fig. 2.24 Effect of uniform field on the various type of particles (positively charged particles, neutral body)

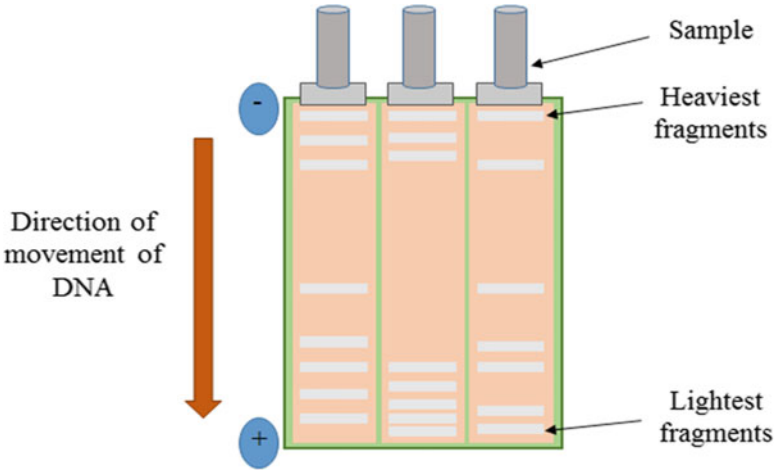

Fig. 2.25 Gel Electrophoresis

moving with the higher speed while longer molecules take more time. In this way separation can be done. If we attach a fluorescence molecule to the DNA being separated, we can exactly get the count of number of molecules with a particular size by counting the fluorescence. Figure 2.25 shows the schematic of gel electrophoresis.

(b) **Capillary Electrophoresis**

Capillary electrophoresis method also shares the similar principle as that of the gel electrophoresis. The only difference is that in case of gel electrophoresis, there are kind of multiple capillaries (pores through gel) being used for causing electrophoresis, while in case of capillary electrophoresis, there is

only one small opening through which DNA travels, i.e., single capillary and the separation takes place in the similar way.

(c) **Surface electrophoresis**

This technique of electrophoresis is mainly used for handling longer strands of DNA. If the DNA strands are long, there is the problem of making them to travel along agarose or so. Hence to handle the heavier molecules, mainly of the size above 10 kbp (kilo base pair), this technique is used. In this case the friction between surface and DNA strand plays a very major role, while making DNA to move on the surface. Li et al. has reported that the mobility of dsDNA, while moving along the surface is influenced by intensity of the electric field, ionic strength and the migration distance [79]. Going with the modifications, gel free microchannel electrophoresis has also been fabricated by Lee and Kuo [80] for fractionating larger DNA. It was observed that the channel's bottom surface was modified in this process. This process helped in fractionating molecules of size 3.5–21.2 kbp. Ghosh et al. [81] fabricated PDMS micro-channels to make dsDNA to travel along. It was observed that the dsDNA travels along the corner rather than the channel base, with the fast speed. The physics behind the movement in such case was also optimized using molecular dynamics simulation. Hence it was remarked that the orthogonally placed pair of surface channel corners is a more favourable option rather than the flat base. Figure 2.26 shows the schematic of the fabricated device.

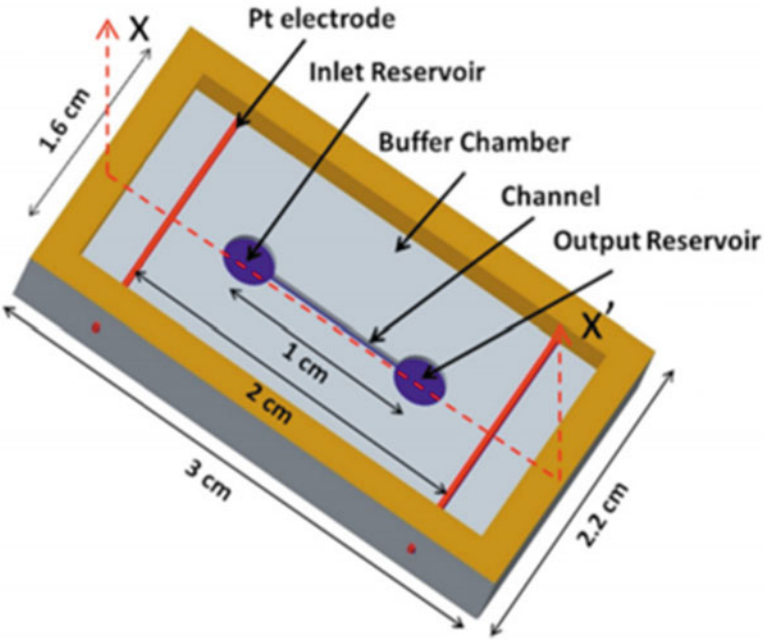

Fig. 2.26 Color online Schematic of the SE device, (dimensions: reservoirs diameter = 3 mm, width of channel = 400 μm, depth of features = 250 μm) (Reproduced from Ghosh et al. [81] with permission from the American Institute of Physics)

5.3 Dielectrophoresis

Dielectrophoresis (DEP) is a phenomenon in which movement of dielectric particles occurs under the effect of force exerted due to non-uniform field. It was demonstrated in 1950s by Herbert Pohl. DEP force depends on various parameters like electrical properties of particle and its surrounding medium, shape and size of dielectric particles and frequency and magnitude of applied field. DEP is helpful in cell separation, cell concentration and nanoparticle/nanowire manipulation. DEP process can be classified in two different types, positive DEP in which dielectrophoresis takes place in the direction of increasing electric field strength and negative DEP in which dielectrophoresis takes place in the direction of reducing field strength. Figure 2.27 shows the effect of non-uniform electric field on the dielectric particles.

DEP force [82] is given by:

$$\mathbf{F_{DEP}} = 2\pi \mathbf{r}^3 \varepsilon_0 \varepsilon_m \mathbf{Re}[\mathbf{K}(\omega)] \nabla \left|\mathbf{E_{rms}}\right|^2 \tag{2.6}$$

Where, r is the radius of the particle, ε_o is permittivity of free space, ε_m is real part of the permittivity of suspending medium, E_{rms} is root mean-square electric field and K(ω) is Clausius-Mossotti factor (measure of effective polarizability of the particle). Clausius-Mossotti factor is given by:

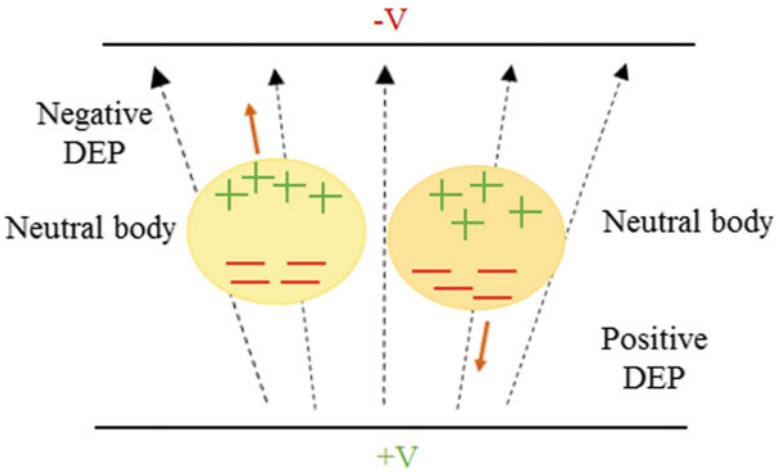

Fig. 2.27 Effect of non-uniform electric field on dielectric particle, positive and negative DEP

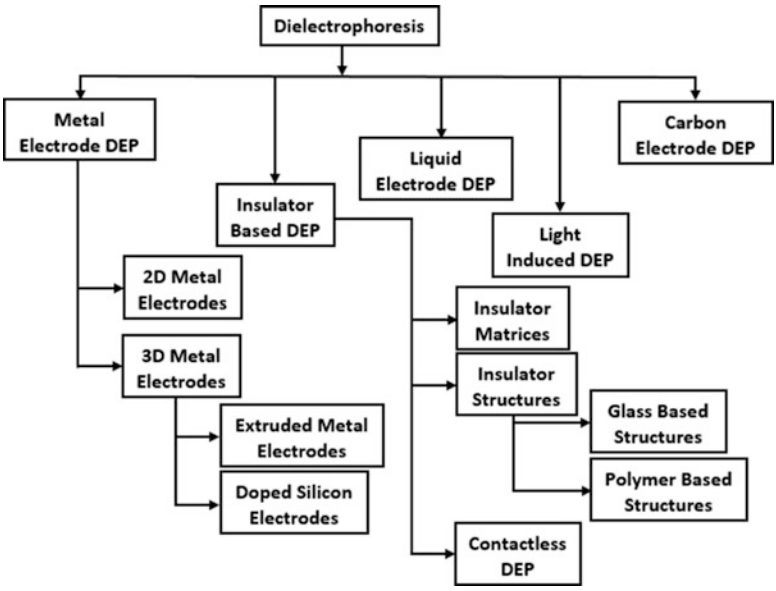

Fig. 2.28 Classification of DEP techniques

$$\mathbf{K}(\boldsymbol{\omega}) = \frac{\left(\boldsymbol{\varepsilon}_{\mathbf{p}}^{*} - \boldsymbol{\varepsilon}_{\mathbf{m}}^{*}\right)}{\left(\boldsymbol{\varepsilon}_{\mathbf{p}}^{*} + \mathbf{2}\boldsymbol{\varepsilon}_{\mathbf{m}}^{*}\right)}; \quad \boldsymbol{\varepsilon}_{(\mathbf{i}=\mathbf{p},\mathbf{m})}^{*} = \boldsymbol{\varepsilon}_{\mathbf{i}} - \mathbf{j}\frac{\boldsymbol{\sigma}_{\mathbf{1}}}{\boldsymbol{\varepsilon}_{\mathbf{0}}\boldsymbol{\omega}} \tag{2.7}$$

Where, p and m refer to the particle and medium, ε is permittivity, σ is conductivity and ω is the angular frequency of applied field ($\omega = 2\pi f$). Dielectrophoresis can be carried out in various circumstances, i.e., using metal electrodes, liquid electrodes, carbon electrode, insulator based DEP and light induced DEP. The detailed classification of the DEP techniques is given in Fig. 2.28.

As Fig. 2.28 represents, DEP can be performed using various types of electrodes, even electrodeless DEP is possible using techniques. Initially metal electrode DEP were used in which metal electrodes used to be printed on the substrate surface. Printed electrodes further possess various characteristics and various designs of electrodes (interdigitated electrodes (IDEs), other discrete shapes etc.) It has advantage of performing the process at low voltage value as the electrodes are placed very near to each other. Very low volume of solution (volume corresponding to ≈ 30 μm height from the base) can effectively undergo DEP process. Beyond this height, the efficiency reduces steeply. In metal electrode category, 2D and 3D types of electrodes are there. 2D electrodes are also called as the planar electrodes. To increase the volume respective to further height, 3D metal electrodes (Extruded metal electrodes, thick layer of doped silicon electrodes) were evolved. With time, several limitations of the metal electrode DEP like constraint on the volume that can undergo DEP and erosion of metal electrodes with time has led to evolution of

Table 2.1 Fabrication techniques for accomplishing DEP

Dielectrophoresis technique		Fabrication techniques	Characteristic features	Problem
Metal electrode DEP [83]	2D metal electrodes	• Metal deposition (Sputtering)	• Voltage requirement: 10 s of volts	Electrode fouling
		• Polymer patterning	• Volume ≈ 30 μm from bottom	
		• Etching		
	3D metal electrodes [84]	• Electrodeposition (Gold electrodes)		
		• Thick film photolithography (Doped Silicon Electrodes [85])		
Insulator based DEP	Insulator matrices [86]		Channel filled with dielectric beads or shapes	Higher voltage requirement
	Insulator structures [87]	• Glass based:	Symmetric repeated insulator structures of various shapes	
		✓ Wet etching		
		• Polymer based [88]:		
		✓ Injection moulding		
		✓ Micromilling		
		✓ Photolithography		
	Contactless DEP [89]		Electrodes not solid but conducting fluid	
Liquid electrode DEP [90]		Metal patterning and polymer photolithography	Vertical equipotential surface creation at side walls	
Light induced DEP [91]			Light excites photoconductive layer and create an electric field gradient	
Carbon electrode DEP [92]			• Low voltage requirement	
			• Lower electrolysis of sample	
			• More chemical stability than metal electrodes	

various new techniques. Table 2.1 represents various fabrication techniques corresponding to the stated techniques along with their characteristics features and problems involved with these modifications.

The characterised DEP modules have been used for various applications, including separation, concentration etc. DEP of various nanoparticles like polystyrene particles and polystyrenes particles mixed with Saccharomyces cerevisiae cells [93] is carried out in asymmetric insulator traps. This kind of DEP has resulted in separation of particles on the basis of size. It was observed that large size particles leave the system earlier than those of the smaller size particles. This separation scheme has been observed valid for individual particles as well as for mixture of cells and polystyrene particles. DEP of DNAs is also carried out by various authors.

Gold IDEs have been used for detecting DNA molecules [94]. A very important remark about the DEP capture of DNA that was observed is DEP capture of DNA takes place in a very specific frequency range. Initially DEP capture increases and at a particular frequency capture stabilizes showing fluorescence plateauing. After this state, DNA capture reduces with increase in frequency. Castle-walled microelectrodes were also used for DEP of DNA [95]. Very interesting observations were made in this study. Below crossover frequency, positive DEP was observed and the DNA capture was seen at the gaps between the printed electrodes. And above crossover frequency, negative DEP was seen and the capture of DNA molecules was seen at the electrodes. It was also emphasized that the crossover frequency changes with change in the length of the DNA molecule. Further applications of DEP are explored in the consequent discussion on PCR in molecular identification.

5.4 Polymerase Chain Reaction Microchips

PCR [96] is the method by which replication of DNA takes place, it is done for some pre-selected sample by conducting a polynucleotide amplification reaction. This is a very useful technique which helps in molecular diagnostics by making several copies of one DNA in very small amount of time. It was discovered in 1985.

For carrying out PCR reaction, a solution has to be prepared which has several component in it like DNA template, primers, Taq-polymerase, Deoxynucleic triphosphates (dNTP's like adenosine (A), cytosine (C), guanine (G), thymine (T)), buffer solution having divalent ions (Mg^{2+} ions) (approximate 1.5 mM concentration in solution, 1:10 dilution). Further a thermal cycler is required to maintain the temperature of the solution in three steps (denaturation, annealing and extension).

Three basic steps of PCR cycle are denaturation (at 94 °C) of dsDNA to two ssDNA, annealing (at 54 °C) of forward and reverse primers to the denatured ssDNA from 5′ to 3′ direction and finally extension (at 7294 °C), attachment of dNTP's and backbone formation by Taq polymerase enzyme. Numbers of cycles that take place in PCR process depend on the quantity of DNA, primers and dNTP's. In general 25–35 cycles are the standard for PCR process. The standard process comprises of denaturing step of 5 min, then 25–35 cycles of 30 s at 9494 °C, 45 s at 5494 °C, 2 min at 7294 °C and final extension of 7 min at 7294 °C.

The basic principle of PCR and thermal cycle steps is elaborated in Fig. 2.29. In PCR, there is exponential increase in number of DNA copies which are generated.

PCR is mainly two types, liquid PCR and solid PCR. Liquid PCR process is the normal PCR process in which all the DNA, primers and dNTP's are in solution. While in solid PCR, primers are immobilized on the surface and DNA and dNTP's remain in the solution above primers. Further there is two amplification mechanism, interfacial amplification and surface amplification that take place in the solid PCR. Optimization of design and fabrication process for inexpensive reusable DNA amplification chip with polydimethylsiloxane chamber (3 μL) on silicon base with spin-on glass layer (140 nm thick) in between is done by Bhattacharya

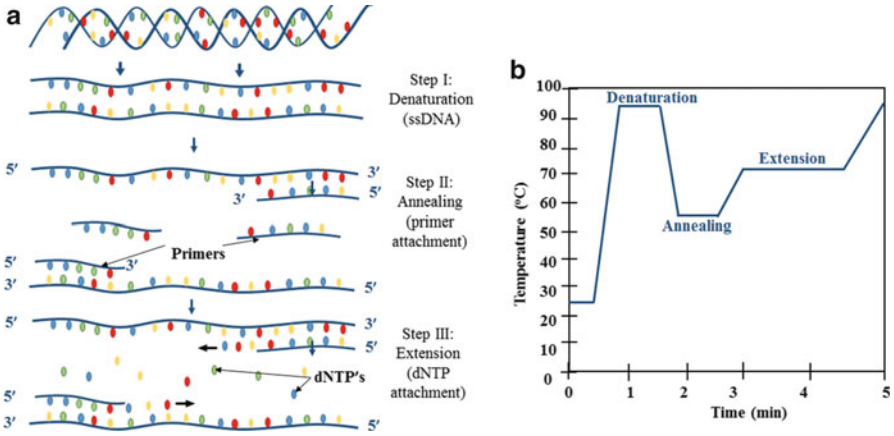

Fig. 2.29 PCR process (**a**) Process description; (**b**) Temperature requirement during PCR process

et al. [97]. Amplification chip contains microfabricated platinum heater structures on the bottom of silicon base. Feed channels and inlet–outlet ports are bonded to SOG film (bond strength: maximum 83 psi) with PCR cycle control by thermal cycle functionalized using sensing thermocouple. 527 fragments of IBR viral genome with 0.07 pg/μL concentration have been amplified in 51 PCR cycles. Figure 2.30 shows the schematic of the fabricated device.

Negligible nonspecific binding of template DNA to the hydrophobic interiors has been shown by fluorescence measurement design. Fabrication of a microchip platform for sensitive detection of microorganisms using integrated sorting; concentration and real time PCR based detection system is done by Nayak et al. [98]. Microchip is designed in such a way that to it pre-concentrates the specific microorganisms from highly dilute sample and real time molecular identification is performed using q-PCR process in a pico-litre micro-channel by use of optimized interdigitated electrodes and micro-scale thermal cycling mechanism. Gold nanoparticles (coated with secondary antibody (Goat anti-mouse IgG)) are attached to targeted microorganisms (E-coli DH5α) to mediate immune-conjugation. Sorting and concentration is done through dielectrophoresis (DEP) technique and finally detection is done by quantitative-PCR (q-PCR) using fluorescence measurement. A primary anti E. coli antibody captured E. coli DH5α cells with binding through nanoparticle bridges. Figure 2.31 shows schematic of detection of molecules.

Fluorescence detection has shown that the DEP frequency is different for the micro-organisms with conjugation and without conjugation. Additionally the fluorescence pattern observed was seen different for in case of conjugated and non-conjugated bacterial cells (Fig. 2.32).

An on-chip system for the electrokinetic capture of bacterial cells and their identification using PCR is designed by Bhattacharya et al. [99] using a PCB

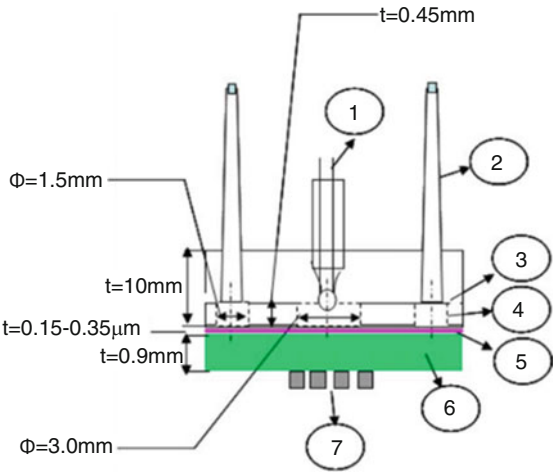

Fig. 2.30 Schematic of the silicon PDMS cassette. (1) Glass housed thermocouple, (2) epoxied inlet/outlet ports, (3) polydimethyl siloxane channels, (4) inlet/outlet reservoirs, (5) SOG layer, (6) thermally oxidized silicon wafer, (7) heaters (Reproduced from Bhattacharya et al. [97] with permission from the Institute of Electrical and Electronics Engineers)

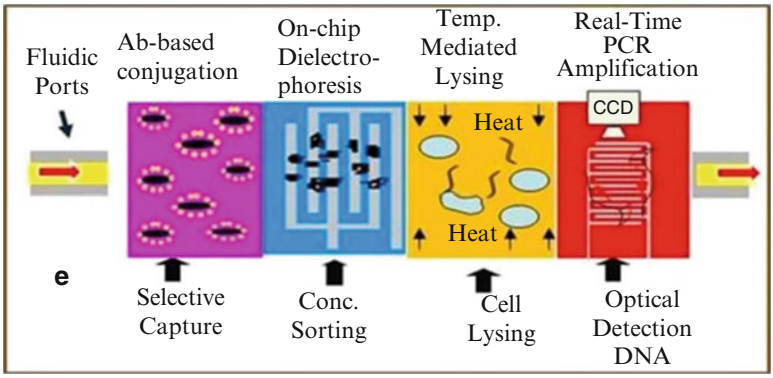

Fig. 2.31 Schematic of detection microorganisms (Reproduced from Nayak et al. [98] with permission from the Nature Publishing Group)

bonded silicon-glass platform with electrodes, micro-channels and chambers built on it is used for identification purpose (Fig. 2.33).

DEP forces are used to divert cells using one set of interdigitated electrodes in big chamber while the diverted cells are collected in smaller chamber with second set of interdigitated electrodes to trap and concentrate the cells. In the trapped cells, under DEP force, PCR mix is injected for PCR amplification with SYBR green detection for identification of Listeria monocytogenes V7 cells. Using DEP forces, higher sensitivity was achieved from 10^6 to 10^4 cfu/mL cells. Very specific identification technique for identifying as low as 60 cells in 600 nL volume. Further optimization of fabrication process for PCR micro-chip through system identification technique is performed [100]. Design and optimal placement of a thin film resistance based temperature detector (RTD) in the PCR microchip is studied and the most optimal design is suggested. RTD integration is done to eliminate the need

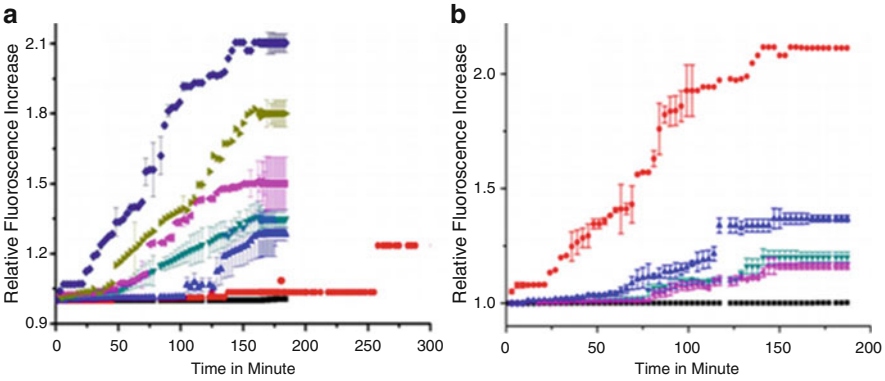

Fig. 2.32 (**a**) Plot showing the trend in increase in fluorescence intensity during DEP of different bacterial cell (normal) concentrations with respect to time, -●-: 10^2 cfu/mL; -▲-: 10^3 cfu/mL; -►-: 10^4 cfu/mL; -▼-: 10^6 cfu/mL; -◄-:10^7 cfu/mL; -◆-: 10^9 cfu/mL; -■-: control, (**b**) Plot showing the trend in increase in fluorescence intensity during DEP of different bacterial cell (conjugated) concentrations with respect to time, -●-: 109 cfu/mL; -▲-:106 cfu/mL; -►-:104 cfu/mL; -▼-: 103 cfu/mL; -■-: control (Reproduced from Nayak et al. [98] with permission from the Nature Publishing Group)

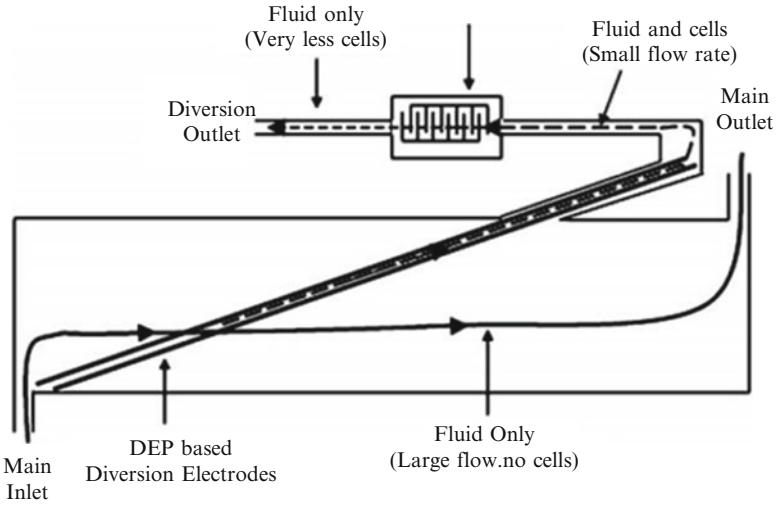

Fig. 2.33 Principle of operation of the dielectrophoresis-based diversion and diversion of cells (Reproduced from Bhattacharya et al. [99] with permission from the Royal Society of Chemistry)

for the thermocouple. In this research the optimal placement test run for placement of RTD is performed. The configuration chosen for RTD placement is heater is placed at the bottom side of the chip while RTD is placed on the upper side of the chip. RTD is used in four wire measurement mode which minimizes measurement errors due to lead resistance. Various placement methods for RTD are studied to obtain a linear relation in input and output parameters. Parametric identification using Auto Regressive with Exogenous Inputs (ARX) method is performed and 2nd

and 4th order temperature models are given which helped in deciding on the final configuration. Detection of DNA is also performed using gold nanoparticle functionalised with primers [101, 102]. Using this type of mechanism, colorimetric change from red to purple is observed, if complementary sequence is present i.e., if hybridization takes place. If hybridization takes place, formation of gold nanoparticle aggregate is observed which is responsible for colour change. This kind of work has also been done by Shen et al. [103] by making some manipulation in the process by immobilising primers on gold nanoparticle surface by thiol bond. Nanostructured aggregate formation on hybridization is observed.

5.5 Gene Delivery Using Nanoscale Material and Electrophoretic Transport of DNA

Gene delivery is the process in which cell is modified by introducing foreign DNA into the cell. This process is very important with respect to gene therapy and genetic modification of crops. Various methods that come into picture while considering gene therapy are viral method (virus has capability to inject its DNA into cell) and non-viral methods (electroporation, microinjection, gene gun, hydrostatic pressure and sonication). Viral method is easy to arrange but it has drawback of having various random insertion sites, while non-viral can be controlled with respect to insertion sites and number of insertions. Various processes have several advantages and respective limitations. Here we are summarizing a bit about electroporation and combination of electroporation and hydrostatic pressure wave method. Electroporation is the method of gene delivery in which high voltage (≈100,000–500,000 V/m) is used for transfecting DNA into cells [104]. This high voltage leads to high transfection but many a times results in high cell mortality as well. Hence if some means can be devised to have higher yield with low electric field strength combined with some other means, it may be a very successful aspect. So in this direction a prominent combination of low electric field (≈20,000 V/m) electroporation and hydrostatic pressure through shock wave is analysed to attain high yield efficiency [105]. This high pressure wave was generated using nano-energetic materials.

6 Various Sensing and Detection Techniques

Interest in BioMEMS has been immensely growing for applications like biosensors for detection of protein/DNA, cells and other biomolecules, immunoisolation devices, drug delivery etc. [106]. There are various detection techniques implemented for signal transduction in biosensors which includes mechanical, electrical and optical primarily. This section presents various BioMEMS sensing modalities.

6.1 Electrochemical Sensing

Electrochemical sensing is one of the oldest techniques used dating back to 1950s. This technique uses electrodes to measure electrical properties to sense materials present in the sample without damaging the sample system. Typically there are several types of electrochemical sensor. The three major types include amperometric, measurement of current, conductometric, measurement of conductive properties and potentiometric, measurement of potential difference or charge accumulation across the electrodes. Impedimetric, which measures impedance change and field-effect, for measurement of current because of the gate potentiometric effect are also, used these days [107].

Amperometric sensors have been typically developed for determination of biochemical oxygen demand (BOD) since conventional techniques take 5–6 days for the measurement. Tonning et al. proposed an interesting approach for sensing of Vibrio fischeri bacterium, Pseudokirchneriellasubcapitata freshwater marine alga and Daphnia magna freshwater crustacean. The fabricated sensor consisted of several cells and electrodes for sensing and finally the data was processed using chemometry mathematical methods [108]. Also, these sensors are commonly used for detection of glucose. Mu et al. investigated nickel oxide modified glucose sensors that use carbon electrodes [109]. These sensors have a response time of 5 s hence demonstrating excellent sensitivity. One of the recent interesting findings include thick-film textile based amperometric sensors. Direct screen printed amperometric sensors incorporated in clothing has been reported by Yang et al. These sensors were printed on the elastic of clothing and studied for mechanical stress, bending and stretching [110]. Specific enzyme sensors can be developed using this technique which can prove useful for the purpose of monitoring alcohol consumption, stress or sweat monitoring for athletes etc.

Microfluidics is commonly used to position cells, but a novel device has been fabricated to trap the cells directly over the sensing electrodes. A microfluidic trap device to measure exocytosis from cells targeting them to electrochemical electrodes has been demonstrated by Gao et al. (Fig. 2.34) [111]. The device is fabricated in a manner such that there is no need for precise pressure control or handling of fluids on the chip.

Conductometric sensors are used in varied fields to measure the change in conductivity of a reaction solution caused by microbial activities. They are preferred over other sensors because of their inexpensive fabrication process, no requirement of reference electrode, high accuracy and cancellation of interferences. In the field of gas sensing, a novel and highly sensitive NO_2 gas sensor using caesium-doped graphene oxide has been reported by Piloto et al. Doping of caesium to graphene oxide results in the carbon atoms reducing the graphene oxide, demonstrating very low detection limits for NO_2 (90 ppb) [112]. Latif and Dickert have

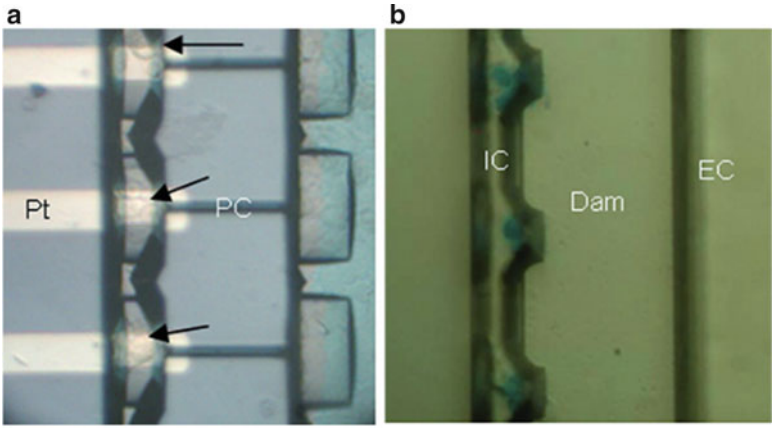

Fig. 2.34 Photomicrographs depicting cells targeted to docking sites (Reproduced from Gao et al. [111] with permission from the Royal Society of Chemistry)

developed a unique conductometric sensor which is a combination of interdigital electrode structures with imprinted polymers for engine's lubricating oil monitoring [113]. Using a sol–gel process, titania and silica are imprinted and used as sensitive coatings. The change of conductance in these layers is measured as they are exposed to varying concentrations of the oil. Conductometric biosensors are extensively used for environmental monitoring as well. They are used for detection of several pollutants, organophosphorous pesticide [114], heavy metal ions [115], formaldehyde [116], 4-chlorophenol [117] and nitrate [118]. In spite of being a novel field, arrays of such sensors can be used for various applications in environmental modeling providing the advantage of improved accuracy and low costs.

Potentiometric sensors work on a principle where an ion-selective or gas sensing electrode is monitored for changes in potential with respect to a reference electrode. When biological molecules bind to the sensing electrode the potential changes due to consumption of the electrolyte by it. Gold coated silicon electrode with alkanethiol molecules immobilized on it is used as a sensing element for detection of cancer and proteins [119]. Real-time wearable sensors are paving their way in owing to their self-tracking nature. From tracking heart rate to monitoring one's mood these sensors help the person quantify their health and make improvements accordingly. A unique tattoo based epidermal pH ion-selective sensor has been developed [120]. It is a flexible wearable sensor which can be an asset for physiological monitoring purposes. Potentiometric sensors are targeting ultra-low cost and robust sensors, which has led to development of paper based potentiometric sensors. Bendable electronics and carbon nanotubes have been combined to develop a novel low-cost sensor for diagnostic purposes which entails advantages like excellent electrical properties, better conductivity and higher surface area contact with the sample [121].

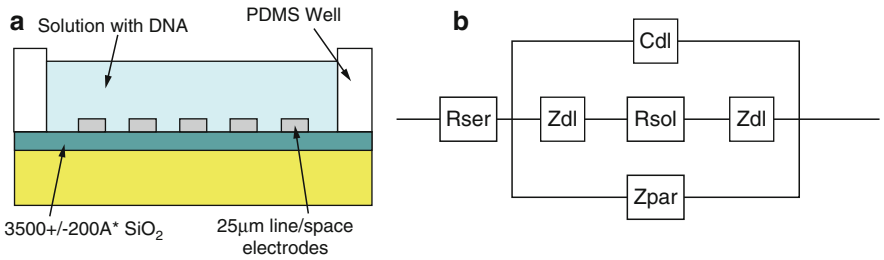

Fig. 2.35 (**a**) Schematic of the sensing device (**b**) Equivalent circuit model of solution with DNA molecules (Reproduced from Liu et al. [123] with permission from the American Institute of Physics)

Impedimetric sensors measure the changes in impedance when biomolecules bind to the electrode hindering the electron transfer. Based on this, carbon electrodes deposited with PBA-modified graphene oxide were reported for detection of glycated haemoglobin (HbA1c) for diagnosis of diabetes [122].

Liu et al. reported a device for label-free electrical detection of DNA through impedance measurement (Fig. 2.35). Impedance vs. frequency characteristic was extracted to detect the presence of DNA molecules in a nanomolar range for a 400 bp molecule [123]. Such electrochemical sensors have great potential for point-of-care diagnostic devices, providing low-cost, high precision and portability.

6.2 Optical Sensing

In the recent decade optical biosensors have drawn extensive attention and have rapidly developed changing the face of communication technologies. Due to its advantages like high sensitivity, low-weight, high capacity to transfer information, invulnerability to electromagnetic interference and low-cost, varied applications are integrating these sensors [124]. The sensing mechanism works on the basis of changes in optical properties such as UV–Vis absorption, bio or chemiluminescence, reflectance and fluorescence brought by the interaction of the biocatalyst with the target analyte [125].

A SU8 based optical biosensor has been reported by Yardi et al. A novel technique has been developed to tag standalone optical fibres to a substrate using laser exposed SU8 micro-droplet (Fig. 2.36). The stitched optical fibres show high transmissibility for both aligned and misaligned configurations of the fibres [126].

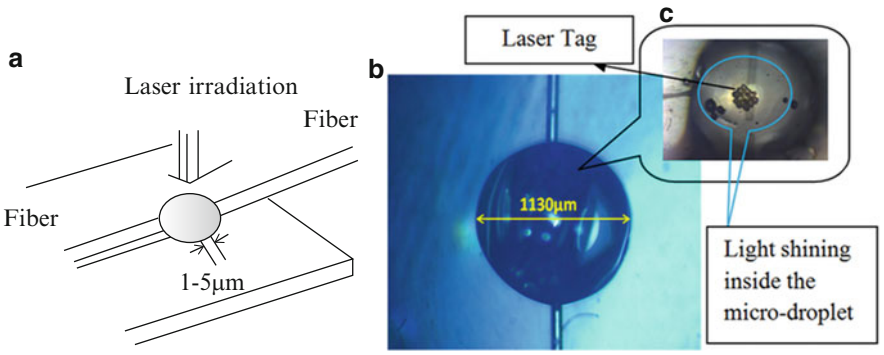

Fig. 2.36 (**a**) Schematic of fibers connected to SU8 droplet (**b**) Optical micrograph of the SU8 droplet (**c**) Image of light shining in the droplet (**c**) Image of light shining in the droplet (Reproduced from Yardi et al. [126], manuscipt accepted and under publising in Springer)

6.3 Mass Based Sensing

Mass based sensors rely on transduction of mechanical energy. Cantilever based mass sensors are the most commonly used mechanical sensors that measure changes in mass through its oscillating frequency shift. Cantilevers came to use as highly sensitive biosensors after the advent of atomic force microscopy (AFM) [127]. They were used as a tip in AFM to measure the force between the tip and the sample through tip deflection or changes in resonant frequency of a vibrating cantilever. A micro-cantilever mass based sensor works on the same principles as above. Interaction of the cantilever with biomolecules changes the resonant frequency of the cantilever [128]. There exists a linear relationship between the added mass and the shift in the resonant frequency of the cantilever. The sensitivity of these devices can be increased by increasing the quality factor, decreasing the mass of the cantilever and using highly sensitive detection instruments to measure small variations in frequency. Several fields like communication, sensing, optics, optical microscopy etc. extensively use these cantilever based devices.

Nano-cantilevers have been reported with detection limits in the range of zeptograms (10^{-21} g) for top-down technology and yoctograms (10^{-24} g) for bottom-up technologies [129]. Nano-cantilever based sensors have reduced sensitivity in liquids due to large damping. A novel sensing mechanism which uses excitation of higher vibration modes to increase the sensitivity has been reported by Braun et al. Bacterial virus T5 interactions were observed using this gold coated cantilever in parallel to measurements at the reference cantilever [130]. Using this mechanism, the quality factor has been increased from 1 (at the 1st mode) to 30 (at 16th mode). Naik et al. have demonstrated high frequency cantilever-based resonators for biomolecular spectrometry. IgM protein was detected in real-time by observing the jumps in the resonance frequency as the protein gets adsorbed onto the cantilever one by one [131]. Utilization of amplitude shift instead of a resonant

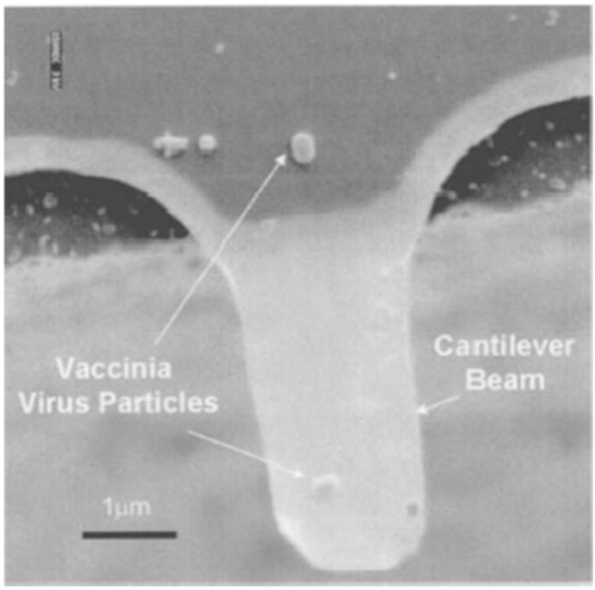

Fig. 2.37 SEM image showing the cantilever with a vaccinia virus particle (Reproduced from Gupta et al. [133] with permission from the American Institute of Physics)

frequency shift to increase the sensitivity and eliminate the frequency tracking elements from the sensor has been reported by Kumar et al. [132].

Gupta et al. used silicon cantilevers to detect bacterial cells (Listeria cells) and viruses (vaccinia virus) (Fig. 2.37). Single virus detection was carried out on 4–5 μm long, 1–2 μm wide and 20–30 nm thick cantilevers [133, 134]. Detection of Bacillus anthracis spores in air and water using a planar rectangular shaped cantilever was demonstrated by Davilia et al. [135].

BioMEMS have made a significant impact on clinical diagnostics and the affordability of these devices. They are being used for detection of protein, DNA, detection of cancer, HIV and other infectious diseases. They have enabled low-cost, rapid and point-of-care diagnostic of diseases allowing early and better diagnosis.

References

1. Whitesides GM (2006) The origins and the future of microfluidics. Nature 442 (7101):368–373
2. Fair RB (2007) Digital microfluidics: is a true lab-on-a-chip possible? Microfluid Nanofluid 3 (3):245–281
3. Srinivasan V, Pamula V, Fair R (2004) An integrated digital microfluidic lab-on-a-chip for clinical diagnostics on human physiological fluids. Lab Chip 4:30–315
4. http://www.drdo.gov.in/drdo/data/Laser%20and%20its%20Applications
5. Robert M, Rossier J, Bercier P, Girault H (1997) UV laser machined polymer substrates for the development of microdiagnostic systems. Anal Chem 69:2035
6. Hellaman A, Rau K, Yoon H, Bae S, Palmer J, Philips K, Albritton N, Venugopal V (2007) Laser-induced mixing in microfluidic channels. Anal Chem 79:4484–4492

7. Quinto-Su PA, Lai HH, Yoon HH, Sims CE, Allbritton NL, Venugopalan V (2008) Examination of laser microbeam cell lysis in a PDMS microfluidic channel using time-resolved imaging. Lab Chip 8(3):408–414
8. Cheng J, Wei C, Hsu C, Young T (2004) Direct-write laser micromachining and universal surface modification of PMMA for device development. Sens Actuators 99:186
9. Klank H, Kutter J, Geschke O (2002) CO(2)-laser micromachining and back-end processing for rapid production of PMMA-based microfluidic systems. Lab Chip 2:242
10. Lippert T, Wei J, Wokaun A, Hoogen N, Nuyken O (2000) Polymers designed for laser microstructuring. Appl Surf Sci 168:270
11. Kant R, Gupta A, Bhattacharya S (2015) Studies on CO2 laser micromachining on PMMA to fabricate microchannels for microfluidic applications. In: 5th international and 26th All India Manufacturing Technology, Design and Research Conference (AIMTDR 2014) December 12th–14th, 2014, IIT Guwahati, Assam, India
12. Johnson T, Waddell E, Kramer G, Locascio L (2001) Chemical mapping of hot-embossed and UV-laser-ablated microchannels in poly(methyl methacrylate) using carboxylate specific fluorescent probes. *Applied Surface Science* 181:149–159
13. Terasawa T (1989) 0.3 μm optical lithography using phase-shifting mask. In: Proceedings of SPIE, p 142
14. Lu Y (2006) A digital micro-mirror device-based system for the micro fabrication of complex, spatially patterned tissue engineering scaffolds. J Biomed Mater Res A 77:396–405
15. Apte P, Rizvi NH (2002) Developments in laser micro-machining techniques. J Mater Process Technol 127:206–210
16. Kumar A, Gupta A, Kant R, Akhtar SN, Tiwari N, Ramkumar J, Bhattacharya S (2013) Optimizaton of laser machining processes for the preparation of photomasks, and its application to microsystem fabrication. J Micro/Nnolith MEMS and MOEMS 13(1):1–8
17. https://www.memsnet.org/mems/processes/lithography.html
18. Whitesides G, Ostuni E, Takayama S, Jiang X, Ingber D (2001) Soft lithography in biology and biochemistry. Ann Rev Biomed Eng 33:335–373
19. Duffy D, Mcdonald J, Schueller O, Whitesides G (1998) Rapid prototyping of microfluidic system in PDMS. Anal Chem 70:4974–4984
20. McDonald J, Duffy D, Anderson J, Chiu D, Wu H, Schueller O, Whitesides G (2000) Fabrication of microfluidic systems in poly(dimethylsiloxane). Electrophoresis 21:27–40
21. Folch A, Toner M (2000) Microengineering of cellular interaction. Ann Rev Biomed Eng 2:227–256
22. Ismagilov R, Rosmarin D, Kenis P, Chiu D, Zhang W, Stone H, Whitesides G (2001) Pressure-driven laminar flow in tangential microchannels: an elastomeric microfluidic switch. Anal Chem 73:4682–4687
23. Chou S, Krauss P, Renstrom P (1996) Nanoimprint lithography. J Vac Sci Technol B 14:4129
24. Whitesides S, Whitesides G (2000) Fabrication of topologically complex three-dimensional microfluidic systems in PDMS by rapid prototyping. Anal Chem 72:3158–3164
25. Singh RK, Ghubade A, Basu B, Bhattacharya S (2009) A novel replicamoulding process for realizing three dimensional microchannels within soft materials. In: ICEMS
26. Singh RK (2014) Micro-manufacturing of 2/3 dimensional
27. Singh RK, Kant R, Pandey SS, Asfer M, Bhattacharya B, Panigrahi PK, Bhattacharya S (2013) Passive vibration damping using polymer pads with microchannel arrays. Microelectromech Syst 22(3):695–707
28. Rajeev Kumar Singh AGSB (2013) Design and fabrication of 3-dimensional helical structure in polydimethysiloxane for flow control applications. Microsyst Technol, pp 1–11
29. Singh RK, Kant R, Singh S, Suresh E, Gupta A, Bhattacharya S (2015) A novel helical microvalve for embedded micro-fluidic applications. Microfluid Nanofluid 19(1):19–29
30. Singh RK, Ghubade A, Chaudhury R, Bhattacharya S (2009) Fabrication technology forbiomedical systems using non-conventional micromachining

31. Osborn JL, Barry L, Elain L, Peter K (2010) Microfluidics without pumps: reinventing the T-sensor and H-filter in paper networks. Lab Chip 10(20):2659–2665
32. Bhattacharya S, Jordan B, Darryl J, Gangopadhyay S (2003) A flow visualization experiment for a first course in micro-fluidics. In: Proceedings of ASEE, University of Texas at Arlington, TX
33. Nguyen N-T, Wu Z (2005) Micromixers—a review. J Micromech Microeng 15:R1–R16
34. Nam-Trung N, Wu Z (2004) Micromixers—a review. J Micromech Microeng 15(2):1–16
35. Kant R, Singh H, Bhattacharya S Nano-scale particle etching using micro-mixer. Microfluid Nanofluid, Manuscript under review
36. Zhang X, Jiang XN, Sun C (1999) Micro-stereolithography of polymeric and ceramic microstructures. Sens Actuators A 77(2):149–156
37. Richard BG, Hahn EL (1975) Coherent two-photon processes: transient and steady-state cases. Phys Rev A 11(5):1641
38. Choudhary R, Bhakat T, Singh RK, Ghubade A, Mandal S, Ghosh A, Rammohan A, Sharma A, Bhattacharya S (2011) Bilayer staggered herringbone micro-mixers with symmetric and asymmetric. J Microfluid Nanofluid 10:271–286
39. Smits JG (1990) Piezoelectric micropump with three valves working peristaltically. Sens Actuators A21–A23:203–206
40. Trouchet D, Ajdari A, Tabeling P, Goulpeau J (2005) Experimental study and modeling of polydimethylsiloxane peristaltic micropumps. J Appl Phys 98:044914
41. Stemme E, Stemme G (1993) A valveless diffuser/nozzle-based fluid. Sens Actuators 39:159–167
42. Carrozza M, Croce N, Magnani B, Dario P (1995) A piezoelectricdriven stereolithography-fabricated micropump. J Micromech Microeng 5:177–179
43. Böhm S, Timmer B, Olthuis W, Bergveld P (2002) A closed-loop controlled electrochemically actuated micro-dosing system. J Micromech Microeng 10:498–504
44. Jeong O, Park S, Yang S, Pak J (2005) Fabrication of a Peristaltic PDMS micro pump. Sens Actuators 123:453–458
45. Kant R, Singh H, Nayak M, Bhattacharya S (2013) Optimization of design and characterization of a novel micro-pumping system with peristaltic motion. Microsyst Technol 19 (4):563–575
46. Atwe A, Gupta A, Kant R, Das M, Sharma I, Bhattacharya S (2014) A novel microfluidic switch for pH control using Chitosan based hydrogels. Microsyst Technol 20(7):1373–1381
47. Singh RK, Kumar A, Kant R, Gupta A, Suresh E, Bhattacharya S (2014) Design and fabrication of 3-dimensional helical structures in polydimethylsiloxane for flow control applications. Microsyst Technol 20(1):101–111
48. Ghoshdastider S, Barizuddin S, Dweik M, Almasri M (2013) A micromachined impedance biosensor for accurate and rapid detection of E. coli O157: H7. RSC Adv 3(48):26297–26306
49. Boehm A, Gottlieb P, Hua S (2007) On-chip microfluidic biosensor for bacterial detection and identification. Sens Actuators B 126(2):508–514
50. Campbell GA, Mutharasan R (2005) Detection and quantification of proteins using self-excited PZT-glass millimeter-sized cantilever. Biosens Bioelectron 21(4):597–607
51. Weeks B, Camarero J, Noy A, Miller A, Yoreo JD (2003) Development of a microcantilever-based pathogen detector. In: Nanotech
52. Ilic B, Yang Y, Craighead H (2004) Virus detection using nanoelectromechanical devices. Appl Phys Lett 85(13):2604–2606
53. Ilic B, Czaplewski D, Zalalutdinov M, Craighead H, Neuzil P, Campagnolo C, Batt C (2001) Single cell detection with micromechanical oscillators. J Vac Sci Technol 19(6):2825–2828
54. Basu AK, Bhattacharya S (2016) Fabrication and resilience measurement of thin aluminium cantilevers using scanning probe microscopy. Taylor and Francis, London
55. Yan G, Chan PC, Hsing I et al (2001) An improved TMAH Si-etching solution without attacking exposed aluminum. Sens Actuator 89:135–141

56. Basu AK, Dwivedi P, Bhattacharya S (2016) Fabrication of 3-dimensional interdigited structure in microfluidic channel by one step maskless greyscale lithography. In: Bangalore India Nano, Bangalore
57. Chen Y-H, Kuo ZK, Cheng C-M (2015) Paper—a potential platform in pharmaceutical development. Trends Biotechnol 33(1):4–9
58. Cheng CM, Martinez AW, Gong J, Mace CR, Phillips ST, Carrilho E, Mirica KA, Whitesides GM (2010) Paper-based ELISA. Angew Chem 49:4771–4774
59. Nie J, Zhang Y, Lin L, Zhou C, Li H, Zhang L, Li J (2012) Low-cost fabrication of paper-based microfluidic devices by one-step plotting. Anal Chem 84(15):6331–6335
60. Li X, Tian J, Nguyen T, Shen W (2008) Paper-based microfluidic devices by plasma treatment. Anal Chem 80:9131–9134
61. Dungchai W, Chailapakul O, Henry C (2011) A low-cost, simple, and rapid fabrication method for paper-based microfluidics using wax screen-printing. Analyst 136(1):77–82
62. Li X, Tian J, Garnier G, Shen W (2010) Fabrication of paper-based microfluidic sensors by printing. Colloid Surf B 76(2):564–570
63. Olkkonen J, Lehtinen K, Erho T (2010) Flexographically printed fluidic structures in paper. Anal Chem 82:10246–10250
64. Chitnis G, Ding Z, Chang C-L, Savran CA, Ziaie B (2011) Laser-treated hydrophobic paper: an inexpensive microfluidic platform. Lab Chip 11:1161–1165
65. Zhang Y, Bai J, Ying JY (2015) A stacking flow immunoassay for the detection of dengue-specific immunoglobulins in salivary fluid. Lab Chip 15:1465–1471
66. Koesdjojo MT, Pengpumkiat S, Wu Y, Boonloed A, Huynh D, Remcho TP, Remcho VT (2015) Cost effective paper-based colorimetric microfluidic devices and mobile phone camera readers for the classroom. J Chem Educ 92:737–741
67. Unicef (2007) Malaria diagnosis: a guide for selecting rapid diagnostic test (RDT) kits
68. Pereira DY, Chiu RY, Zhang SC, Wu BM, Kamei DT (2015) Single-step, paper-based concentration and detection of a malaria biomarker. Anal Chim Acta 882:83–89
69. Weaver AA, Lieberman M (2015) Paper test cards for presumptive testing of very low quality antimalarial medications. Am Soc Tropical Med Hygiene 92:17–23
70. Cordray MS, Kortum RRR (2015) A paper and plastic device for the combined isothermal amplification and lateral flow detection of Plasmodium DNA. Malar J 14:1
71. Kumar A, Hens A, Arun RK, Chatterjee M, Mahato K, Layek K, Chanda N (2015) A paper based microfluidic device for easy detection of uric acid using positively charged gold nanoparticles. Analyst 140:1817–1821
72. Teoh BT, Sam SS, Tan KK, Danlami MB, Shu MH, Johari J, Hooi PS, Brooks D, Piepenburg O, Nentwich O, Smith AW, Franco L, Tenorio A, AbuBakar S (2015) Early detection of dengue virus by use of reverse transcription recombinase polymerase amplification. J Clin Microbiol 53:830–837
73. Yen C-W, Puig HD, Tam JO, Márquez JG, Bosch I, Schifferli KH, Gehrke L (2015) Multicolored silver nanoparticles for multiplexed disease diagnostics: distinguishing dengue, yellow fever, and Ebola viruses. Lab Chip 15:1638–1641
74. Lo S-J, Yang S-C, Yao D-J, Chen J-H, Tu W-C, Cheng C-M (2013) Molecular-level dengue fever diagnostic devices made. Lab Chip 13:2686–2692
75. Hamraoui A, Nylander T (2002) Analytical approach for the Lucas–Washburn equation. J Colloid Interface Sci 250:415–421
76. Byrnes S, Thiessen G, Fu E (2013) Progress in the development of paper-based diagnostics for low-resource point-of-care settings. Bioanalysis 5:2821–2836
77. Fu E, Ramsey SA, Kauffman P, Lutz B, Yager P (2011) Transport in two-dimensional paper networks. Microfluid Nanofluid 10:29–35
78. Mansfield MA (2005) The use of nitrocellulose membranes in lateral-flow assays. In: Drugs of abuse. Springer, New York, pp 71–85
79. Li B, Fang X, Luo H, Peterson E, Seo Y-S, Samuilov V, Rafailovich M, Sokolov J, Gersappe D, Chu B (2006) Influence of electric field intensity, ionic strength, and migration

distance on the mobility and diffusion in DNA surface electrophoresis. Electrophoresis 27 (7):1312–1321
80. Lee HH, Kuo Y (2008) Surface modification of Gel-Free microchannel surface electrophoresis device for DNA identification. Jpn J Appl Phys 47(4R):2300
81. Ghosh A, Patra TK, Kant R, Singh RK, Singh JK, Bhattacharya S (2011) Surface electrophoresis of ds-DNA across orthogonal pair of surfaces. Appl Phys Lett 98(16):164102
82. Jones TB, Jones TB (2005) Electromechanics of particles. Cambridge University Press, Cambridge
83. Price JA, Burt JP, Pethig R (1988) Applications of a new optical technique for measuring the dielectrophoretic behaviour of micro-organisms. Biochim Biophys Acta 964(2):221–230
84. Voldman J, Gray ML, Toner M, Schmidt MA (2002) A microfabrication-based dynamic array cytometer. Anal Chem 74(16):3984–3990
85. Iliescu C, Xu GL, Samper V, Tay FE (2004) Fabrication of a dielectrophoretic chip with 3D silicon electrodes. J Micromech Microeng 15(3):494
86. Lin IJ, Benguigui L (1982) High-intensity, high-gradient electric separation and dielectric filtration of particulate and granular materials. J Electrostat 13(3):257–278
87. Chou C-F, Tegenfeldt JO, Bakajin O, Chan SS, Cox EC, Darnton N, Duke T, Austin RH (2002) Electrodeless dielectrophoresis of single-and double-stranded DNA. Biophys J 83 (4):2170–2179
88. McGraw GJ, Davalos RV, Brazzle JD, Hachman JT, Hunter MC, Chames JM, Fiechtner GJ, Cummings EB, Fintschenko Y, Simmons BA (2005) Polymeric microfluidic devices for the monitoring and separation of water-borne pathogens utilizing insulative dielectrophoresis. In: MOEMS-MEMS Micro and Nanofabrication, pp 59–68
89. Shafiee H, Caldwell JL, Sano MB, Davalos RV (2009) Contactless dielectrophoresis: a new technique for cell manipulation. Biomed Microdevices 11(5):997–1006
90. Demierre N, Braschler T, Muller R, Renaud P (2008) Focusing and continuous separation of cells in a microfluidic device using lateral dielectrophoresis. Sens Actuators B 132 (2):388–396
91. Hoeb M, Radler JO, Klein S, Stutzmann M, Brandt MS (2007) Light-induced dielectrophoretic manipulation of DNA. Biophys J 93(3):1032–1038
92. Jaramillo MC, Torrents E, Martin-Duarte R, Madou MJ, Juarez A (2010) On-line separation of bacterial cells by carbon-electrode dielectrophoresis. Electrophoresis 31(17):2921–2928
93. Saucedo-Espinosa MA, LaLonde A, Gencoglu A, Romero-Creel MF, Dolas JR, Lapizco-Encinas BH (2016) Dielectrophoretic manipulation of particle mixtures employing asymmetric insulating posts. Electrophoresis 37(2):282–290
94. Bakewell DJ, Morgan H (2006) Dielectrophoresis of DNA: time-and frequency-dependent collections on microelectrodes. IEEE Trans NanoBiosci 5(1):1–8
95. Kasahara H, Ding Z, Nakano M, Suehiro J (2015) Effect of DNA length on dielectrophoretic characteristics of DNA-labeled microbeads. In: IEEE international conference on industrial technology, pp 3341–3346
96. Wilding P, Kricka LJ (1996) Polymerase chain reaction. U.S. Patent 5,587,128, 24
97. Bhattacharya S, Gao Y, Korampally V, Othman MT, Grant S, Kleiboeker SB, Gangopadhyay K, Gangopadhyay S (2007) Optimization of design and fabrication processes for realization of a PDMS-SOG-silicon DNA amplification chip. J Microelectromech Syst 16 (2):401–410
98. Nayak M, Singh D, Singh H, Kant R, Gupta A, Pandey SS, Mandal S, Ramanathan G, Bhattacharya S (2013) Integrated sorting, concentration and real time PCR based detection system for sensitive detection of microorganisms. Sci Rep 3:3266
99. Bhattacharya S, Salamat S, Morisette D, Banada P, Akin D, Liu Y-S, Bhunia AK, Ladisch M, Bashir R (2008) PCR-based detection in a micro-fabricated platform. Lab Chip 8 (7):1130–1136
100. Korampally V, Bhattacharya S, Gao Y, Grant S, Kleiboeker SB, Gangopadhyay K, Tan J, Gangopadhyay S (2006) Optimization of fabrication process for a PDMS-SOG-Silicon based

PCR Micro Chip through system identification techniques. In: IEEE international symposium on computer-based medical system, pp 329–334
101. Cai M, Li F, Zhang Y, Wang Q (2010) One-pot polymerase chain reaction with gold nanoparticles for rapid and ultrasensitive DNA detection. Nano Res 3(8):557–563
102. Deng H, Xu Y, Liu Y, Che Z, Guo H, Shan S, Sun Y, Liu X, Huang K, Ma X, Wu Y (2012) Gold nanoparticles with asymmetric polymerase chain reaction for colorimetric detection of DNA sequence. Anal Chem 84(3):1253–1258
103. Shen H, Hu M, Yang Z, Wang C, Zhu L (2005) Polymerase chain reaction of Au nanoparticle-bound primers. Chin Sci Bullet 50(18):2016–2020
104. Zimmerman U, Pilwat G, Riemann F (1974) Dielectric breakdown of cell membranes. In Membrane transport in plants, pp 146–153
105. Patel VK, Kant R, Bhatt G, Ganguli A, Singh D, Nayak M, Gupta A, Gangopadhyay K, Gangopadhyay S, Gurunath R, Bhattacharya S Synchronized electro-mechanical shock wave induced bacterial transformation, Paper under review
106. Grayson A, Shawgo R, Johnson A, Flynn N, Li Y, Cima M (2004) A BioMEMS review: MEMS technology for physiologically integrated devices. Proc IEEE 92:6–21
107. Grieshaber D, MacKenzie R, Voeroes J, Reimhult E (2008) Electrochemical biosensors-sensor principles and architectures. Sensors 8:1400–1458
108. Ponomareva O, Arlyapov V, Alferov V, Reshetilov A (2011) Microbial biosensors for detection of biological oxygen demand (a Review). Appl Biochem Microbiol 47:1–11
109. Mu Y, Jia D, He Y, Miao Y, Wu H (2011) Nano nickel oxide modified non-enzymatic glucose sensors with enhanced sensitivity through an electrochemical process strategy at high potential. Biosens Bioelectron 26:2948–2952
110. Yang Y, Chuang M, Lou S, Wang J (2010) Thick-film textile-based amperometric sensors and biosensors. Analyst 135:1230–1234
111. Gao Y, Bhattacharya S, Chen X, Barizuddin S, Gangopadhyay S, Gillis K (2009) A microfluidic cell trap device for automated measurement of quantal catecholamine release from cells. Lab Chip 9:3442–3446
112. Piloto C, Notarianni M, Shafiei M, Taran E, Galpaya D, Yan C (2014) Highly NO2 sensitive caesium doped graphene oxide conductometric sensors. Beilstein J Nanotechnol 5:1073–1081
113. Latif U, Dickert F (2011) Conductometric sensors for monitoring degradation of automotive engine oil. Sensors 11:8611–8625
114. Dzydevich S, Shul'ga A, Soldatkin A, Nyamsi Hendji A, Jaffrezic-Renault N, Martelet C (1994) Application of conductometric for sensitive detection of pesticides biosensor based on the cholinesterases. Electroanalysis 6:752–758
115. Zhylyak G, Dzyadevich S, Korpan Y, Soldatkin A, El'Skaya A (1995) Application of urease conductometric biosensor for heavy-metal ion determination. Sens Actuators B 24:145–148
116. Soldatkin A, Dzyadevich S, Korpan Y, Arkhipova V, Zhylyak G, Piletsky S (1998) Biosensors based on conductometric detection. Biopolymers Cell 14:268
117. Anh T, Dzyadevych S, Van M, Renault N, Duc C, Chovelon J (2004) Conductometric tyrosinase biosensor for the detection of diuron, atrazine and its main metabolites. Talanta 63:365–370
118. Xuejiang W, Dzyadevych S, Chovelon J, Renault N, Ling C, Siqing X (2006) Conductometric nitrate biosensor based on methyl viologen/Nafion®/nitrate reductase interdigitated electrodes. Talanta 69:450–455
119. Wang Y, Zhang Z, Jain V, Yi J, Mueller S, Sokolov J (2010) Potentiometric sensors based on surface molecular imprinting: detection of cancer biomarkers and viruses. Sens Actuators B 146:381–387
120. Bandodkar A, Hung V, Jia W, Valdés-Ramírez G, Windmiller J, Martinez A (2013) Tattoo-based potentiometric ion-selective sensors for epidermal pH monitoring. Analyst 138:123–128

121. Novell M, Parrilla M, Crespo G, Rius F, Andrade F (2012) Paper-based ion-selective potentiometric sensors. Anal Chem 84:4695–4702
122. Siva Rama Krishna V, Bhat N, Amrutur B, Chakrapani K, Sampath S (2011) Detection of glycated hemoglobin using 3-aminophenylboronic acid modified graphene oxide. Life Science Systems and Applications Workshop (LiSSA), 2011 IEEE/NIH, pp 1–4
123. Liu Y, Banada P, Bhattacharya S, Bhunia A, Bashir R (2008) Electrical characterization of DNA molecules in solution using impedance measurements. Appl Phys Lett 92:143902
124. Yang M, Li S, Jiang D (2014) Review on optical fiber sensing technologies for industrical applications at the NEL-FOST. In: EWSHM-7th European workshop on structural health monitoring
125. Bhattacharya S, Jang J, Yang L, Akin D, Bashir R (2007) BioMEMS and nanotechnology-based approaches for rapid detection of biological entities. J Rapid Meth Automat Microbiol 15:1–32
126. Seema Yardi A, Kant R, Boolchandani D, Bhattacharya S (2015) High efficiency coupling of optical fibres with SU8 micro-droplet using laser welding process. Lasers in manufacturing and materials processing, pp 1–17
127. Binnig G, Quate C, Gerber C (1986) Atomic force microscope. Phys Rev Lett 56:930
128. Lavrik N, Sepaniak M, Datskos P (2004) Cantilever transducers as a platform for chemical and biological sensors. Rev Sci Instrum 75:2229–2253
129. Tamayo J, Kosaka P, Kosaka J, San Paulo A, Calleja M (2013) Biosensors based on nanomechanical systems. Chem Soc Rev 42:1287–1311
130. Braun T, Ghatkesar M, Backmann N, Grange W, Boulanger P, Letellier L (2009) Quantitative time-resolved measurement of membrane protein–ligand interactions using microcantilever array sensors. Nat Nanotechnol 4:179–185
131. Naik A, Hanay M, Hiebert W, Feng X, Roukes M (2009) Towards single-molecule nanomechanical mass spectrometry. Nat Nanotechnol 4:445–450
132. Kumar V, Boley W, Yang Y, Ekowaluyo H, Miller J, Chiu G (2011) Bifurcation-based mass sensing using piezoelectrically-actuated microcantilevers. Appl Phys Lett 98:153510
133. Gupta A, Akin D, Bashir R (2004) Single virus particle mass detection using microresonators with nanoscale thickness. Appl Phys Lett 84:1976–1978
134. Gupta A, Akin D, Bashir R (2004) Detection of bacterial cells and antibodies using surface micromachined thin silicon cantilever resonators. J Vacuum Sci Technol B 22:2785–2791
135. Davila A, Jang J, Gupta A, Walter T, Aronson A, Bashir R (2007) Microresonator mass sensors for detection of Bacillus anthracis Sterne spores in air and water. Biosens Bioelectron 22:3028–3035